

A novel mechanism for regulating the activity of proliferating cell nuclear antigen by a small protein

Zhuo Li¹, Richard Y.-C. Huang^{1,2}, Daniel C. Yopp³, Travis H. Hileman³, Thomas J. Santangelo³, Jerard Hurwitz⁴, Jeffrey W. Hudgens^{1,2} and Zvi Kelman^{1,2,*†}

¹Institute for Bioscience and Biotechnology Research, 9600 Gudelsky Drive, Rockville, MD 20850, USA, ²National Institute of Standards and Technology, 9600 Gudelsky Drive, Rockville, MD 20850, USA, ³Department of Microbiology and Center for RNA Biology, Ohio State University, Columbus, OH 43210, USA and ⁴Program of Molecular Biology, Memorial Sloan Kettering Cancer Center, 1275 York Avenue, New York, NY 10065, USA

Received December 29, 2013; Revised March 06, 2014; Accepted March 10, 2014

ABSTRACT

Proliferating cell nuclear antigen (PCNA) forms a trimeric ring that associates with and influences the activity of many proteins participating in DNA metabolic processes and cell cycle progression. Previously, an uncharacterized small protein, encoded by TK0808 in the archaeon *Thermococcus kodakarensis*, was shown to stably interact with PCNA *in vivo*. Here, we show that this protein, designated Thermococcales inhibitor of PCNA (TIP), binds to PCNA *in vitro* and inhibits PCNA-dependent activities likely by preventing PCNA trimerization. Using hydrogen/deuterium exchange mass spectrometry and site-directed mutagenesis, the interacting regions of PCNA and TIP were identified. Most proteins bind to PCNA via a PCNA-interacting peptide (PIP) motif that interacts with the inter domain connecting loop (IDCL) on PCNA. TIP, however, lacks any known PCNA-interacting motif, suggesting a new mechanism for PCNA binding and regulation of PCNA-dependent activities, which may support the development of a new subclass of therapeutic biomolecules for inhibiting PCNA.

INTRODUCTION

Proliferating cell nuclear antigen (PCNA) plays essential roles in DNA metabolic processes such as replication, repair, recombination and cell cycle progression [reviewed in (1–3)]. PCNA monomers form a ring-shaped trimer that encircles duplex DNA (4,5) and tethers other enzymes to the DNA (1,6,7). To date, all activities described for PCNA

proteins require them to encircle the duplex; no biochemical function for PCNA off DNA has been reported. This suggests that mechanisms or regulatory factors that limit PCNA assembly could exert significant control of PCNA-dependent activities *in vivo*. Furthermore, most PCNA proteins form stable rings that cannot independently assemble around the duplex. Replication factor C (RFC) complex functions as the clamp loader and assembles the PCNA rings around the duplex [reviewed in (8)].

Most of the proteins that interact with PCNA do so via a PIP (PCNA-interacting peptide) motif (9,10). The PIP motif is a fairly weak consensus sequence of QXXhXXaa where ‘h’ is a moderately hydrophobic amino acid (isoleucine, leucine or methionine) and ‘a’ is an aromatic residue, followed by a non-conserved sequence containing basic amino acids. The PIP motif interacts with the loop that connects the two domains in each PCNA monomer [referred to as interdomain connecting loop (IDCL)] (11). Biochemical and structural analyses illustrated requirements for an intact PIP motif for the interactions between PCNA and different proteins. Another less common motif involved in PCNA binding is the KA motif (12,13). This motif is found in a small subset of PCNA interacting enzymes, usually in conjunction with a canonical PIP motif. It is not clear where this motif binds on the PCNA ring. However, as the C-terminus of PCNA is also required for its interaction with other proteins [e.g. (14,15)] it was suggested that the KA motif might interact with that region. Other minor PCNA-binding motifs have also been reported [e.g. the AlkB homologue 2 PCNA-interacting motif, APIM (16)].

This use of a PIP-like motif appears, at least partially, conserved in bacteria. The β -subunit is the functional homologue of PCNA in bacteria and also forms a ring-shaped

*To whom correspondence should be addressed. Tel: (240) 314-6294; Fax: (240) 314-6255; Email: zkelman@umd.edu

†Zvi Kelman would like to dedicate the paper to the memory of Rolf Bernander, a pioneer in the study of the archaeal cell cycle, a colleague and a friend.

Present addresses:

Zhuo Li, Third Institute of Oceanography, State Oceanic Administration, 184 Daxue Road, Xiamen, Fujian 361005, China.

Richard Y.-C. Huang, Bristol-Myers Squibb, Route 206 and Province Line Road, Princeton, NJ 08543, USA.

Thomas J. Santangelo, Department of Biochemistry and Molecular Biology, Colorado State University, Fort Collins, CO 80523, USA.

structure that encircles double stranded DNA (17). Similar to PCNA, the β -subunit interacts with a number of enzymes involved in nucleic acid metabolic processes. Many of these enzymes bind to the β -subunit via consensus sequences, QL[S/D]LF and QLxLx[L/F], which resemble the PIP motif (18,19).

Genes encoding for PCNA are present in all archaeal genomes and while the genomes of most euryarchaeota contain a single gene encoding PCNA, the genome of *Thermococcus kodakarensis* contains two genes encoding PCNA homologues (TK0535 and TK0582, encoding PCNA1 and PCNA2, respectively) (20–22). It was found that both proteins form homotrimeric structures with characteristics similar to those of other archaeal and eukaryal PCNA proteins (20,23). Both proteins were also shown to support processive DNA synthesis by DNA polymerase B (PolB) and polymerase D (PolD) (20–22).

Many archaeal replication proteins were identified by their homology to the eukaryotic or bacterial counterparts using *in silico* approaches. Bioinformatic tools, however, cannot identify archaeal-specific replication proteins or proteins without conserved sequences. In the last few years, however, genetic tools have been used to expand the pool of putative archaeal replication factors. In one of these studies, several established replication proteins from the archaeon *T. kodakarensis* were tagged *in vivo* with an amino- or carboxy-terminal hexahistidine extension (His-tag) (24). These proteins were purified from *T. kodakarensis* cell lysates using nickel-affinity columns, and the proteins that co-isolated were identified (24).

One of the proteins identified in the study was a small protein (~8.5 kDa) encoded by TK0808 that co-purified with PCNA1 (24). The protein, however, does not contain a canonical PIP motif, any other motif known to participate in PCNA interaction, or sequence similarity to proteins interacting with the bacterial β -subunit. Bioinformatic analysis revealed that homologous proteins are present only in Thermococcales genomes. *In vitro* studies reported here show that the protein encoded by TK0808 could bind both PCNA1 and PCNA2 resulting in the inhibition of PCNA-dependent activities of a DNA polymerase and flap endonuclease 1 (Fen1). Therefore, the protein was designated TIP (Thermococcales, including Pyrococci and Thermococci, inhibitor of PCNA). We applied an orthogonal approach that uses hydrogen/deuterium exchange mass spectrometry (HDX-MS) and site-directed mutagenesis to locate the regions on PCNA and TIP that drive their binding interactions. We demonstrate that TIP does not interact with the C-terminal part of PCNA or with the IDCL of the PCNA molecule, consistent with the lack of canonical PIP motif. Instead, our experimental data identified different epitopes on the TIP and PCNA proteins involved in protein–protein interaction. It was found that binding of TIP to PCNA facilitates the dissociation of the PCNA trimer and suppresses PCNA activity. The study may provide a new target for drug discovery through TIP derivatives.

MATERIALS AND METHODS

Cloning and purification of recombinant proteins

For protein expression in *Escherichia coli*, the genes encoding TIP (TK0808) and Fen1 (TK1281) were PCR-amplified from *T. kodakarensis* genomic DNA using primers that include NdeI and SalI restriction enzymes in the forward and reverse primers, respectively (Supplementary Table S1). The amplified DNA was ligated with pET15b to introduce an in-frame His₆-tag at the N-terminus of each protein (25). All constructs were sequenced to insure the integrity of the sequence. The construction of the expression vectors for *T. kodakarensis* PCNA1, PCNA2, RFC, PolB and *Methanothermobacter thermoautotrophicus* PCNA (mtPCNA) has been previously described (20,21,26,27).

Vectors that express the mutant forms of PCNA2 (PCNA2-A, K197A-Y200A-Y204A and PCNA2-E, K197E-Y200E-Y204E) were generated by site-specific mutagenesis using a QuikChange kit (Agilent Technologies) with plasmids that encode the wild-type proteins as templates, and oligonucleotides listed in Supplementary Table S1. The vector to express the monomeric form of PCNA1 (PCNA1m, E143K-V175D-I177K) was generated by site-specific mutagenesis using a QuikChange kit (Agilent Technologies) in two stages with plasmid that encode the wild-type protein as the first template, and the oligonucleotides listed in Supplementary Table S1. First the E143K mutant was introduced, followed by the introduction of the V175D-I177K double mutant. The vector to express the monomeric form of PCNA2 (PCNA2m, R75A-F111E-R143A) and mtPCNA (mtPCNAm, D141K-A173D-I175K) was synthesized and cloned into pET21a by Polepolar Technologies.

The pET-based vectors encoding the different proteins were transformed into BL21 DE3 Rosetta cells (Life Technologies) and protein expressions were induced at 37°C by the addition of 0.5 mM IPTG and further incubation for 3 h. The proteins were purified by adsorption to and elution from a Ni²⁺-column, as previously described for the PCNA proteins (20). All proteins were, at least, 95% pure as judged by polyacrylamide-sodium dodecyl sulphate (SDS) gel. Following purification, the proteins were aliquoted and stored at –80°C.

Size exclusion chromatography

Aliquots of each experimental protein (100 μ g) or protein mixtures (100 μ g each) and Gel Filtration standards (Bio-Rad) were dissolved in 200 μ l of 25 mM Tris–HCl (pH 8.0), 200 mM NaCl, 0.5 mM EDTA and 10% (v/v) glycerol and loaded onto a Superdex-200 column (HR10/30; GE Healthcare) pre-equilibrated in the same buffer. Fractions (250 μ l) were collected from the column at a flow rate of 0.5 ml/min. The proteins present in aliquots (80 μ l) of each fraction were separated by electrophoresis through a 15% (w/v) polyacrylamide-SDS gel and stained with Coomassie brilliant blue (R250).

Elongation assay of singly primed M13

PolB catalyzed elongation of singly primed M13 ssDNA was carried out in reaction mixtures (20 μ l) containing 40 mM Tris-HCl (pH 8.0), 250 mM NaCl, 1.5 mM dithiothreitol (DTT), 100 μ g/ml bovine serum albumin (BSA), 10 mM magnesium acetate, 2 mM ATP, 100 μ M each of dCTP, dGTP, and dTTP, 20 μ M [α - 32 P]dATP (1.2×10^4 cpm/pmol), 10 fmol of singly primed M13mp18, 440 fmol of RFC and 100 fmol of PolB and PCNA1, PCNA2 and TIP proteins were added as indicated in the figure legend. Reaction mixtures were incubated for 20 min at 70°C. Following incubation, reactions were treated with 2 μ l of stop solution (containing 0.1 M ethylenediaminetetraacetic acid (EDTA), 5% SDS, 80 μ g yeast tRNA, 20 μ g proteinase K) and incubated for 20 min at 37°C. For quantitation, aliquots (4 μ l) of reaction mixtures were removed, and DNA synthesis measured by adsorption to DE81 paper followed by washings and liquid scintillation counting. The mixture was adjusted to 3 M ammonium acetate and 70% ethanol and the DNA collected by centrifugation. Following *in vacuo* drying the pellets were dissolved in 0.05 M NaOH and 1 mM EDTA and separated by alkaline agarose electrophoresis.

Fen1 nuclease assay

Three oligonucleotides were used to generate the substrate for Fen1 assays. H7 (5'-CTTCAATCGGCTCAGACC GAGCAGAATTCTATGTGTTTACCAAGCGCTG-3') was labeled at the 5'-end with 32 P using [γ - 32 P]ATP and polynucleotide kinase. Following the labeling the DNA was hybridized to two additional oligonucleotides, H2 (5'-CAGCGCTTGGTAAACACATAGAATTCTGCT CGGTCTCTCGGCAGATTCTAGAAATCGACGCT AGCAAGTGAC-3') and H5 (5'-GTCACCTGCTAGCG TCGATTTCTAGAATCTGCCGAG-3'). The substrate was purified from a polyacrylamide gel as previously described (28).

Unless otherwise noted, Fen1 nuclease assays were performed in 20 μ l reactions containing 20 fmol substrates, 25 mM Tris-HCl (pH 8.0), 10 mM MgCl₂, 125 μ g/ml BSA, and proteins as indicated in the figure legends. Reactions were incubated at 60°C for 1 h. Following incubation, reactions were stopped by adding 20 μ l of 95% formamide, 10 mM EDTA and 0.1 \times Tris-Borate-EDTA (TBE) followed by incubation at 100°C for 2 min. The reaction products were separated on 20% polyacrylamide-8 M urea gels in 1 \times TBE followed by visualization and quantification using phosphorimaging (GE Healthcare).

Thermococcus kodakarensis strain construction and confirmation of genome structures

Thermococcus kodakarensis strains were grown in artificial sea water (ASW) with 5 g/l each of yeast extract (Y) and tryptone (T), and 2 g/l sulfur (S^o) at 85°C with the growth of cultures measured by an increase in optical density at 600 nm (OD_{600 nm}) as previously described (29). Plasmids pOSU0808A, pOSU0808B and pOSU0808D were created using standard molecular biology techniques and maintained in *E. coli* (29). Transformation of *T. kodakarensis*

cells (30) and strain construction for markerless deletion of the TK0808 gene were performed as previously described (29). Strains were constructed by transformation of *T. kodakarensis* TS559 (29), with transformants grown on media lacking agmatine for plasmid incorporation, and then counter-selected on media containing 6-methylpurine to generate a strain containing the deletion of TK0808 with no selectable marker (29). The TK0808 open reading frame (ORF) contains 195 bp. The THH2 strain (Δ TK0808) was generated by deleting the first 189 bp of the TK0808 ORF. The last 6 bp of the TK0808 ORF overlap with the TK0807 gene and were thus retained in the chromosome and not deleted.

pTHH6 construction and confirmation

Sequences encoding TIP were amplified via PCR with a 5' primer that contained the promoter for histone B from *M. thermautotrophicus* (P_{hmtB}). The resultant amplicon was cloned into pTS543 (31) at a unique NotI restriction site using Clonotech In-Fusion[®] HD cloning.

Southern blot analysis

The genomic organization of strain THH2 was confirmed via Southern blots of Acc65I and BglII-digested genomic DNA. The Acc65I and BglII restriction fragments that hybridized to a digoxigenin (DIG)-labeled amplicon probe, PCR-generated from within TK0808 (probe B/C) and a flanking region (probe E/F) (Figure 5), were identified using anti-DIG antibodies coupled to alkaline phosphatase as previously described (32).

Thermococcus kodakarensis growth curves

Thermococcus kodakarensis strains were grown overnight in 5 ml ASW YTS^o medium, and strains lacking pTHH6 were supplemented with 1 mM agmatine sulfate. Growth at 85°C of triplicate cultures was monitored at OD_{600 nm} of 1:100 dilutions of inoculated cultures.

Sensitivity to ultraviolet light irradiation, methyl methanesulfonate and mitomycin C

Strains were exposed to DNA damaging agents essentially as previously described (33). Briefly, aliquots (5 μ l) of serial dilutions of cells sampled from growing cultures of *T. kodakarensis* TS559 and THH2 (Δ TK0808) were plated, under anaerobic conditions, on ASW-S^o medium containing all 20 amino acids and 1 mM agmatine, plus or minus 0.1% methyl methanesulfonate (MMS) or 100 μ g/ml mitomycin C. The colonies present on each plate, after 60 h incubation at 85°C, were counted. Similarly, aliquots of dilutions of the same cultures were spotted onto ASW-S^o plates containing all 20 amino acids and 1 mM agmatine and were then exposed to ultraviolet (UV) irradiation (model UVH-46550, International Biotechnologies Inc.) for 1 min before the plates were incubated anaerobically at 85°C for 60 h to allow colony formation.

H/D exchange mass spectrometry

For H/D exchange (HDX) mass spectrometry (MS) analyses, the protein stock solution was diluted in PBS buffer (20 mM sodium phosphate, 500 mM NaCl, pH 7.6) to prepare a 15 μ M final analytical concentration and equilibrated at 4°C for 2 h. The PCNA–TIP complex was prepared by mixing PCNA and TIP at a ratio of 1:1 (PCNA monomer:TIP monomer) and equilibrated at 4°C for 16 h.

HDX was conducted on a HDX PAL robot (LEAP Technologies, Carrboro, NC, USA). Protein solutions (5 μ l) were diluted into 21 μ l D₂O buffer (20 mM sodium phosphate, 500 mM NaCl, pD 7.6) at 3°C. This temperature was chosen to slow the H/D exchange rates so that the observed rates better fit the dynamic range of the instrument. At selected times (30 s, 5, 20, 40 and 60 min) the HDX was quenched by mixing with 40 μ l of 3 M urea, 1% trifluoroacetic acid (TFA) at 1°C. The quenched solution was injected into an on-line pepsin-digestion device for 3 min. The digested protein solution was trapped on a C18 guard column (1.0 mm diameter, 5 μ m, Grace Discovery Sciences). The peptide mixture was separated with a C18 analytical column (1.0 mm diameter \times 5 cm length, 1.9 μ m, HyperSIL GOLD, Thermo Scientific) via a Dionex Ultimate 3000 UPLC with a 9.5 min gradient operated with a binary mixture of solvents A and B at 50 μ l/min flow rate. The gradient settings were: 5–35% solvent B in 3 min, 35–70% solvent B in 5 min, 70–100% solvent B in 0.5 min and isocratic flow at 100% solvent B for 0.5 min, then returned to 5% solvent B in 0.5 min. Solvent A was water containing 0.1% formic acid, and solvent B was 80% acetonitrile and 20% water containing 0.1% formic acid. All LC connection lines and valves were housed in the refrigerated compartment of the HDX PAL at 2°C. Peptides were analyzed on a Thermo LTQ Orbitrap Elite (Thermo Fisher, San Jose, CA, USA). The instrument settings were: spray voltage, 3.7 kV; sheath gas flow rate, 25 (arbitrary units); capillary temperature, 270°C. Three replicates were obtained for each ion-exchange time point.

Peptide identification and HDX data processing

Peptides of PCNA (PCNA1, PCNA2, PCNA2-A mutant, PCNA2-E mutant) and TIP were identified using tandem MS (MS/MS) on the Thermo LTQ Orbitrap Elite. One full mass spectral acquisition triggered six scans of MS/MS [precursor ion is activated by collision-induced dissociation (CID)] whereby the most abundant precursor ions were sequenced. Peptide identification was achieved by submitting Thermo RAW files to both MASCOT (Matrix Science, Oxford, UK) and MassMatrix database search engines. The MASCOT settings were: enzyme, none; MS tolerance, 20 ppm; MS/MS tolerance, 0.6 Da; maximum number of missed cleavages, 3; peptide charge of 1+, 2+ and 3+. The MassMatrix settings were: enzyme, nonspecific; precursor ion tolerance, 10 ppm; product ion tolerance, 0.8 Da; minimum pp score, 5.0. All identifications of peptides were manually confirmed. From mass spectra obtained during HDX-MS experiments the centroid of each deuterated peptide envelope and the relative deuterium uptake by each peptide were calculated with HDX Workbench (34). Corrections for back exchange were made by considering the

values of 80% deuterium content of the exchange buffer and an estimated 70% deuterium recovery. Paired *t*-tests, computed by the Prism 5.01 software package (35), were used in verifying the deuterium uptake differences. The quality of the HDX data fixed the threshold for statistical significance at $P < 0.05$.

RESULTS

TIP interacts with PCNA1 and PCNA2 *in vitro*

TIP protein, encoded by TK0808, was co-isolated with His₆-PCNA1 (TK0535) from *T. kodakarensis* cell lysates (24). To determine if the two proteins also interacted *in vitro*, recombinant TIP and PCNA1 were mixed and the products were examined by size exclusion chromatography. As previously reported (21,22), PCNA1 protein (29.1 kDa) elutes as a trimeric complex (Figure 1A; elution peak in fraction 55). TIP (9.8 kDa) alone eluted as a monomer (Figure 1C, elution peak in fraction 67). When incubated together, TIP and PCNA1 interacted to form a complex, as shown by the elution of TIP in earlier fractions (Figure 1D, elution peak in fraction 58) and elution of PCNA1 in later fractions (Figure 1D, elution peak in fraction 58). Each TIP molecule binds to one PCNA monomer as judged by low resolution X-ray structure of the complex (unpublished observation).

As discussed above, the *T. kodakarensis* genome encodes for two PCNA proteins (21,22) with similar overall structures (20). It was reported that PCNA2 is present at low levels *in vivo* [<50 molecules per cell (21,22)], which may explain the inability to detect PCNA2–TIP interaction *in vivo*. Nevertheless, the ability of TIP to interact with PCNA2 was also evaluated. PCNA2 protein (29.3 kDa) elutes as a trimeric complex (Figure 1B; elution peak in fraction 55) as previously reported (21,22). Similar to PCNA1, TIP also forms a complex with PCNA2, as shown by the elution of TIP in earlier fractions than TIP alone (Figure 1E, elution peak in fraction 52), but with significantly lower affinity.

Homologues of TIP have been identified only in the genomes of Thermococcales. This may suggest that only PCNA proteins from these organisms can bind TIP. Therefore, as a control, a PCNA homologue from a different euryarchaeon, *M. thermautotrophicus*, was used. As previously reported (27), the mtPCNA protein (30.4 kDa) elutes from the sizing column as a trimer (Figure 1F; elution peak in fraction 55). The presence of TIP did not affect this elution profile (compare Figure 1G to Figure 1F) and the elution profile of TIP was not altered by the presence of mtPCNA (compare Figure 1G to Figure 1C).

TIP binds to monomeric PCNA

As shown in Figure 1D and E, TIP binds to both PCNA1 and PCNA2. However, in comparison to PCNA1, only a small fraction of TIP co-eluted with PCNA2 (compare Figure 1D to Figure 1E), suggesting a weaker interaction between TIP and PCNA2 than with PCNA1. It was previously shown that PCNA2 forms a more stable trimer than PCNA1 (20,21). It is thus possible that TIP requires an exposed interface on the PCNA ring in order to bind. As PCNA2 is a stable trimer in solution, at any given time only a small fraction of the rings are open and therefore only a

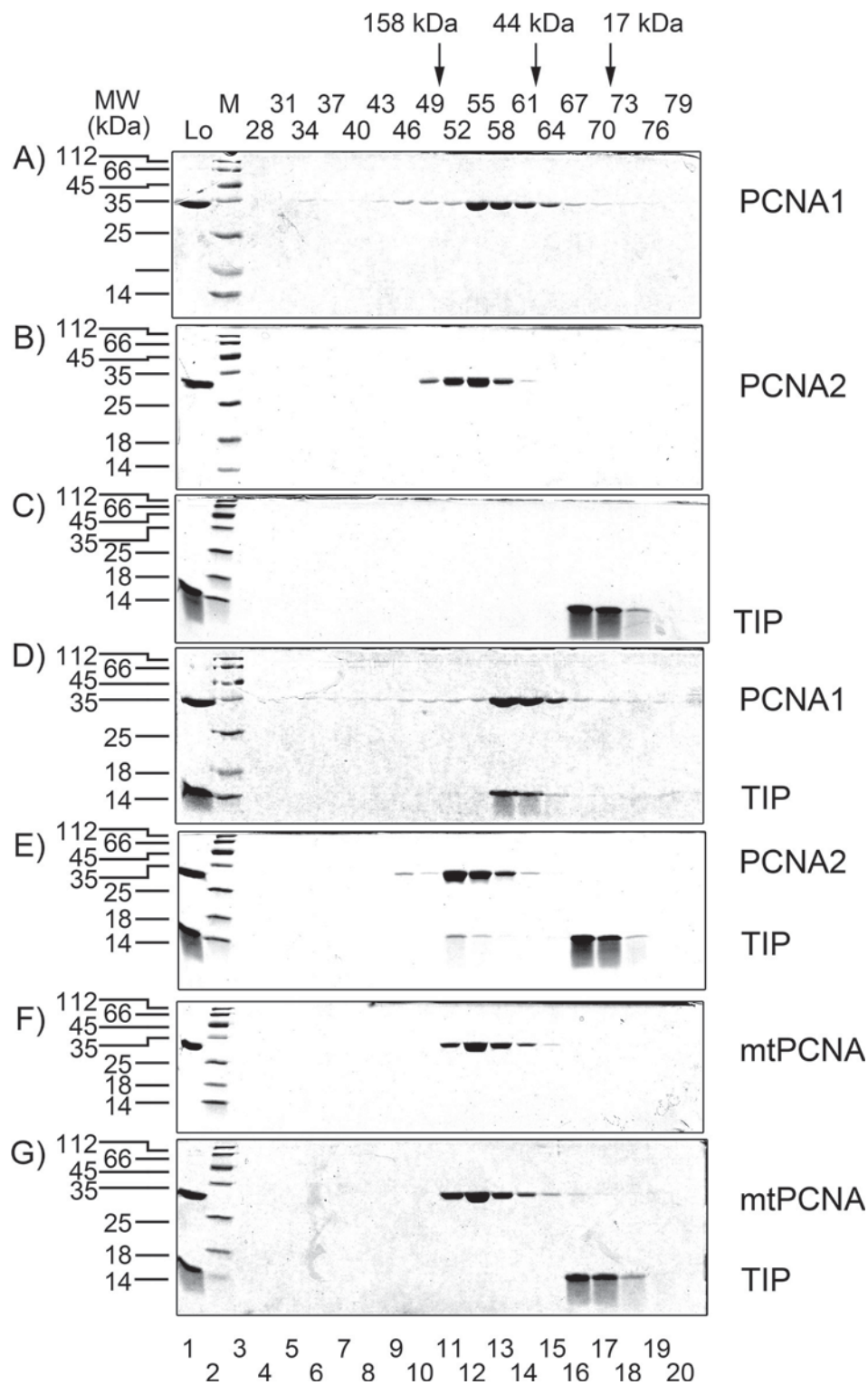


Figure 1. TIP interacts with PCNA1 and PCNA2. Proteins (100 μ g each) were separated on a Superdex-200 gel filtration column as described in 'Materials and Methods' section. Aliquots (80 μ l) from indicated fractions were separated on 15% SDS-PAGE and then stained with Coomassie brilliant blue (R-250). (A) PCNA1; (B) PCNA2; (C) TIP; (D) PCNA1 and TIP; (E) PCNA2 and TIP; (F) mtPCNA; (G) mtPCNA and TIP.

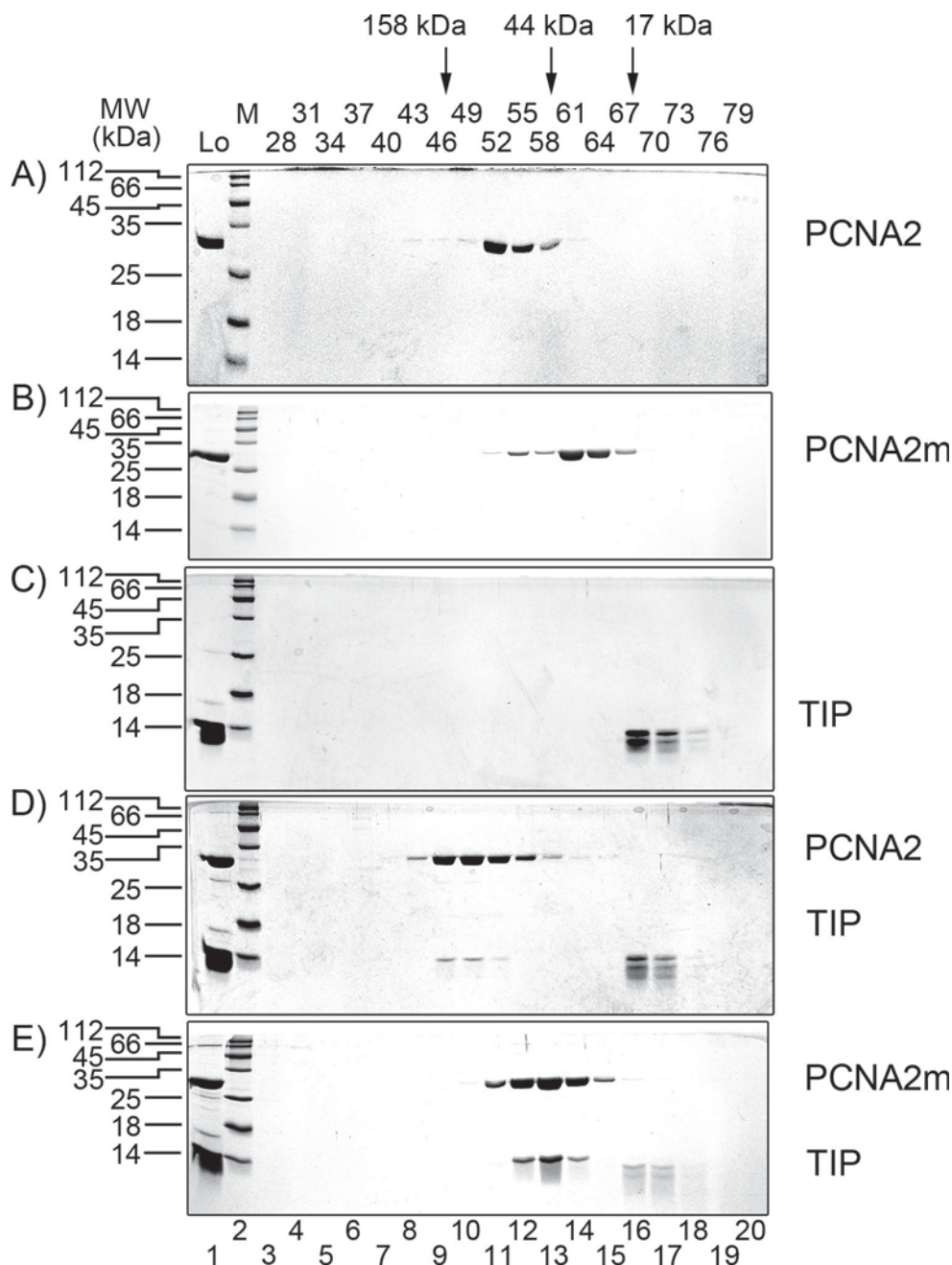


Figure 2. TIP interacts with the monomeric form of PCNA2. Proteins (100 μ g each) were separated on a Superdex-200 gel filtration column as described in 'Materials and Methods' section. Aliquots (80 μ l) from the indicated fractions were separated on 15% SDS-PAGE and stained with Coomassie brilliant blue (R-250). (A) PCNA2; (B) PCNA2m; (C) TIP; (D) PCNA2 and TIP; (E) PCNA2m and TIP.

small subset of the interfaces are exposed and available to bind TIP. This may contribute to the observed weak binding between TIP and PCNA2 (Figure 1E).

To evaluate this possibility, a monomeric form of PCNA2 (PCNA2m) was generated using the PCNA2 structure as a guide (PDB: 3LX2) (20). Three residues in the interfaces between the protomers were mutated (R75A-F111E-R143A) to generate the monomer PCNA2m. TIP binds poorly to PCNA2 as shown by the small amount of TIP-PCNA2 complex formed (Figure 2D, fraction 49). PCNA2m (Figure 2B) and TIP (Figure 2C) are both monomeric (elution

peaks in fraction 61 and fraction 70, respectively). When incubated together, TIP and PCNA2m interacted to form a stable complex as shown by the elution of both proteins as a complex (Figure 2E, elution peak in fraction 58). Taken together with the results presented in Figure 1 and the previous data on the stability of PCNA1 and PCNA2 (20,21), these findings suggest that TIP needs an exposed interface for PCNA binding. However, TIP does not interact with any monomeric PCNA as it does not bind the monomeric form of mtPCNA (mtPCNA_m, Supplementary Figure S1).

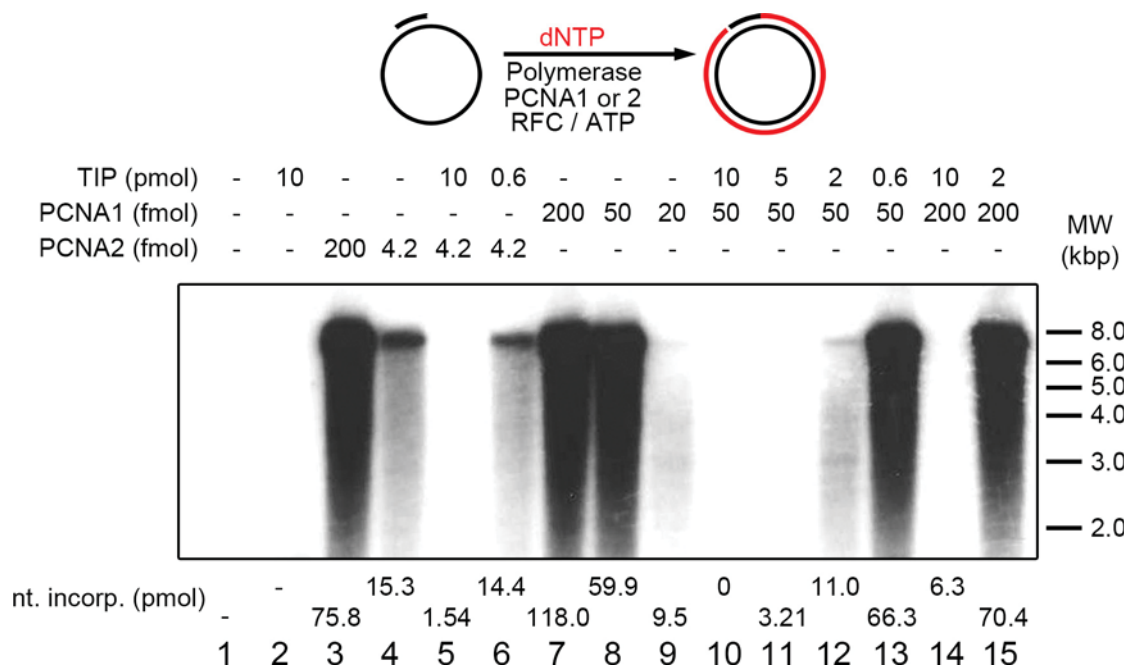


Figure 3. TIP inhibits the PCNA stimulation of PolB. Reaction mixtures (20 μ l) were as described under ‘Materials and Methods’ section in the presence of 200 fmol (lanes 7, 14 and 15), 50 fmol (lanes 8 and 10–13), or 20 fmol (lane 9) of PCNA1 or 200 fmol (lane 3), or 4.2 fmol (lanes 4–6) of PCNA2 in the presence of 0.6 pmol (lanes 6 and 13), 2 pmol (lanes 12 and 15), 5 pmol (lane 11), or 10 pmol (lanes 2, 5, 10 and 14) of TIP. Reactions were incubated for 20 min at 70°C; an aliquot (4 μ l) was used to measure DNA synthesis, and the remaining mixture was subjected to 1.1% alkaline-agarose gel electrophoresis. After drying, gels were autoradiographed for 15 min at –80°C and then developed. The assay is schematically shown at the top.

TIP inhibits PCNA-dependent PolB activity

PCNA proteins bind and stimulate the activity of many proteins involved in nucleic acid metabolic processes. The best understood function for PCNA is its role as the processivity factor for DNA polymerases. While the processivity of replicative polymerases alone is low, the addition of PCNA dramatically increases processive synthesis (8). TIP binding to PCNA may regulate PCNA functions. Therefore, the effect of TIP on PCNA stimulation of PolB activity was evaluated using a singly primed M13 template.

As previously reported (20,21), the elongation of a primed ssM13 template by PolB was detected only in the presence of RFC and either PCNA1 (Figure 3 compare lanes 7–9 to lane 1) or PCNA2 (Figure 3 compare lanes 3 and 4 to lane 1). The presence of TIP, however, inhibited the stimulatory effect of both PCNA proteins (Figure 3 compare lanes 5 and 6 to lane 4; lanes 10–13 to lane 8; and lanes 14 and 15 to lane 7). TIP, without PCNA, did not affect PolB activity (Figure 3 lane 2). It was previously shown that higher concentrations of PCNA1, in comparison to PCNA2, are needed to achieve a similar stimulation of PolB (20,21). This is likely due to the lower stability of PCNA1 trimeric rings (20). Therefore, the concentrations of PCNA1 used in the experiments shown in Figure 3 are higher than those used for PCNA2.

The inhibitory effect of TIP on PCNA-dependent PolB activity could be due to the binding of TIP to PCNA or the binding of TIP to PolB. The ability of TIP to bind PolB and the effect of TIP on PolB–PCNA interactions were evaluated using size exclusion chromatography. TIP (9.8 kDa) alone eluted as a monomer (Supplementary Figure S2C,

elution peak in fraction 67). PolB (89.6 kDa) alone also eluted as a monomer (Supplementary Figure S2D, elution peak in fraction 55). The elution profile did not change when TIP and PolB proteins were incubated together (compare Supplementary Figure S2I to S2C and S2D). PCNA1 (29.1 kDa) and PCNA2 (29.3 kDa) eluted as homotrimers (Supplementary Figure S2A and B; elution peaks in fraction 55). When PCNA1 or PCNA2 were incubated with PolB, they formed a complex (Supplementary Figure S1E and G; elution peaks in fraction 49). When TIP was added to the complex, however, the interactions between PCNA1 and PCNA2 with PolB were inhibited (Supplementary Figure S2F and H) likely due to the PCNA–TIP interactions. These results suggest that the inhibitory effect of TIP on PCNA-dependent processivity of PolB occurs by inhibiting the interactions between PCNA and PolB.

TIP inhibits PCNA-dependent Fen1 activity

In a number of organisms PCNA stimulates the activity of Fen1, a structure-specific nuclease involved in Okazaki fragment maturation (36–38). Fen1 removes the flap structure that contains the RNA primer prior to gap filling by the polymerase and subsequent ligation of the two adjacent Okazaki fragments (36,37). Although the effect of PCNA on Fen1 activity has been shown for other organisms, it has not yet been reported for *T. kodakarensis*. Therefore, the effects of PCNA1 and PCNA2 on Fen1 activity were evaluated using a Fen1 assay (shown schematically in Figure 4A). The experiments were performed in the absence of RFC using the ability of PCNA to thread onto duplex DNA as was previously reported (39). Fen1 alone has weak nu-

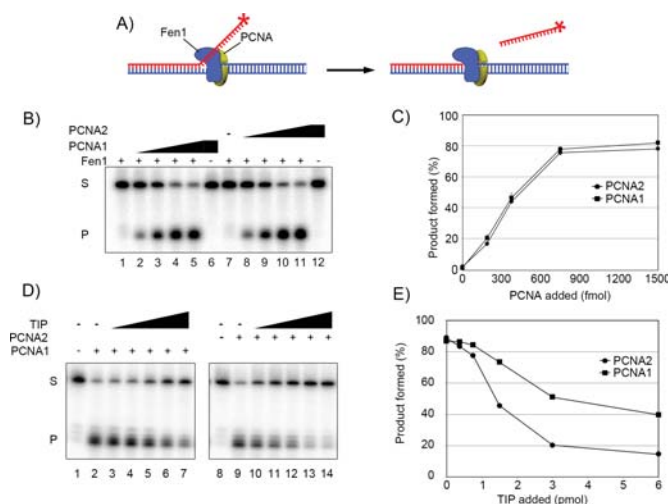


Figure 4. TIP inhibits PCNA stimulation of Fen1 activity. (A) A schematic illustration of the assay. (B and C) The effect of PCNA on Fen1 activity was measured as described in ‘Materials and Methods’ section in a reaction mixture (20 μ l) that contained 20 fmol substrates, 250 fmol Fen1 (lanes 1–5 and 7–11), 188 fmol (lane 2), 375 fmol (lane 3), 750 fmol (lane 4), or 1500 fmol (lanes 5 and 6) of PCNA1, or 188 fmol (lane 8), 375 fmol (lane 9), 750 fmol (lane 10), or 1500 fmol (lanes 11 and 12) of PCNA2. The reactions mixtures were incubated at 60°C for 60 min, and the products were separated on 20% (w/v) polyacrylamide–8 M urea gels, visualized and quantified by phosphorimaging. A representative gel is shown in panel (B), and the average, with standard deviation, from three independent experiments are shown in panel (C). (D and E) The effect of TIP on PCNA stimulation of Fen1 activity was measured as described in ‘Materials and Methods’ section in a reaction mixture (20 μ l) that contained 20 fmol substrates, 250 fmol Fen1, 1500 fmol PCNA1 (lanes 2–7), or 1500 fmol PCNA2 (lanes 9–14) in the presence of 375 fmol (lanes 3 and 10), 750 fmol (lanes 4 and 11), 1500 fmol (lanes 5 and 12), 3000 fmol (lanes 6 and 13), or 6000 fmol (lanes 7 and 14) of TIP. The reaction mixtures were incubated at 60°C for 60 min and the products separated on 20% (w/v) polyacrylamide–8 M urea gels, visualized and quantified by phosphorimaging. A representative gel is shown in panel (D) and the average, with standard deviations from three independent experiments, are shown in panel (E).

cleave activity (Figure 4B lanes 1 and 7) and both PCNA1 (Figure 4B lanes 2–5, also see panel C) and PCNA2 (Figure 4B lanes 8–11, also see panel C) stimulate the activity of Fen1 in a concentration-dependent manner. The concentrations of PCNA used to examine Fen1 stimulation (Figure 4) were higher than those used to stimulate PolB (Figure 3) and therefore at the concentrations tested both PCNA proteins stimulate Fen1 activity to a similar extent (Figure 4B and C). As expected, neither PCNA1 nor PCNA2 alone possess nuclease activity (Figure 4B lanes 6 and 12).

Next, the effect of TIP on Fen1 stimulation by each PCNA protein was evaluated. PCNA-dependent Fen1 activity was inhibited in the presence of TIP in a concentration-dependent manner (Figure 4D compare lanes 3–7 to lane 2; and lanes 10–14 to lane 9, also see panel E). Although both PCNAs stimulate Fen1 activity to a similar extent (Figure 4C), TIP is more efficient in inhibiting the effect of PCNA2 than PCNA1 (Figure 4E). Why TIP appears to be more efficient in inhibiting PCNA2 is not clear especially in light of the stronger binding of TIP to PCNA1 (Figure 1). However, as gel-filtration is not an equilibrium technique, it is possible that under equilibrium conditions TIP binds PCNA2 better than PCNA1. Nevertheless, as

with the effect of TIP on PolB activity, the binding of TIP to PCNA inhibits Fen1 activity.

TIP is not essential for *T. kodakarensis* viability

PCNA is an essential protein and plays critical roles in many nucleic acid transactions. Therefore, one could expect that TIP, which regulates PCNA activity, may also be essential for *T. kodakarensis* viability. To test this hypothesis, we constructed a *T. kodakarensis* strain deleted for the gene encoding TIP, TK0808. *Thermococcus kodakarensis* THH2 (Δ TK0808) was obtained and the genome structure of the mutant confirmed by diagnostic PCR (Figure 5B) and Southern blots (Figure 5C). The growth of the THH2 strain was indistinguishable from the wild-type strain (Figure 5D), suggesting that TIP is not essential for *T. kodakarensis* viability under normal growth conditions. As the PCNA protein also plays an essential role in DNA repair (3), the THH2 strain was evaluated for its sensitivity to the DNA damaging agents including UV, MMS and mitomycin C. No substantial differences were detected between the wild-type and Δ TK0808 strains (data not shown).

Protein dynamics of PCNA and TIP

While the structures of both PCNA proteins from *T. kodakarensis* are known (20), the structure of TIP is not. One approach to understand the structural properties of these two partners is by studying their conformational dynamics in solution. Measurements of peptide-level HDX kinetics can potentially reveal protein dynamics in solution with a spatial resolution of 6–10 residues (40). To attain such resolution, proteolysis of the subject proteins during the HDX-MS measurements must efficiently produce a distribution of peptides of overlapping sequence and leave negligible levels of the parent protein. Immobilized pepsin digested PCNA2 efficiently, but failed to adequately digest PCNA1 for study (Supplementary Figure S3); hence, our HDX-MS studies focused on the PCNA2 system. Proteolytic digestion of native PCNA2 and TIP with pepsin yielded HDX information for 98% of the PCNA2 backbone and 99% of the TIP backbone (Supplementary Figure S4).

The higher order structure of TIP is unknown. As shown by the HDX-MS exchange rate heat map of TIP (Figure 6A), amide groups of TIP, especially in the C-terminal half of the molecule, rapidly exchange to contain over 80% deuterium within the first 30 s after dilution in D₂O. Such fast conformational dynamics are in accord with the view that TIP is mostly unstructured, as has also been suggested by NMR analysis (data not shown).

When the dynamic structure of PCNA2 based on our HDX-MS kinetic data was mapped onto the crystal structure of PCNA2 (PDB: 3LX2) (20), it showed that the interior–helical regions near the trimeric interfaces are structurally stable (Figure 6B), as they exchanged an extremely low amount of deuterium over durations ranging from seconds to hours. On the other hand, the outer helices and loop regions, which are closed to the trimeric interfaces, are relatively more flexible, as their amide sites exchanged substantial levels of deuterium on a time scale of 20 min at 3°C (Figure 6B). The exterior, long-loop regions were less

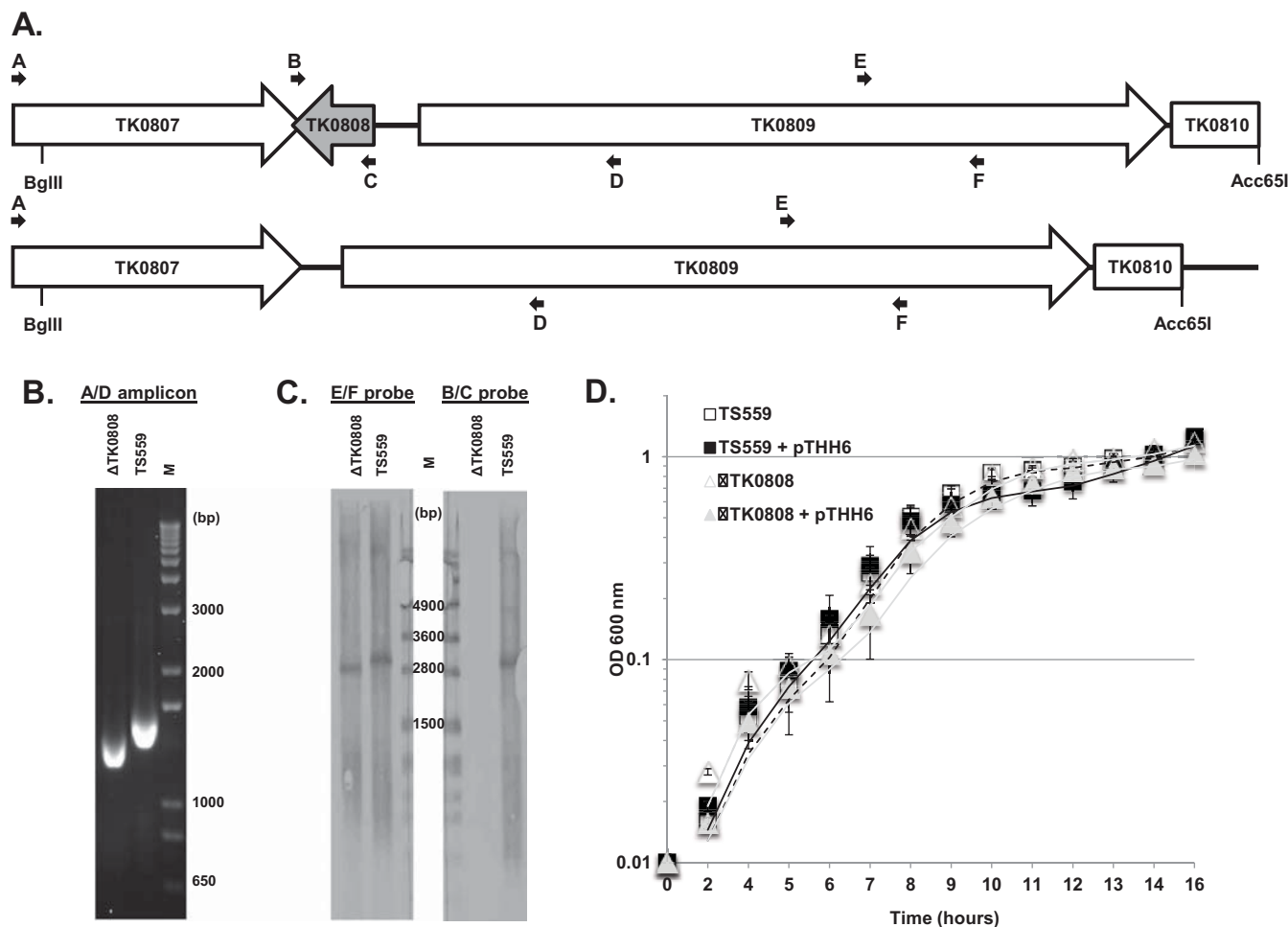


Figure 5. TIP is not essential for *Thermococcus kodakarensis* viability. (A) Annotated sections of the *T. kodakarensis* strains TS559 (top) and Δ TK0808 (bottom) genomes, highlighting the locations of genes (open arrows) and oligonucleotide primers (black arrows; labeled A–F). The approximate locations of relevant Acc65I and BglIII restriction sites are shown. (B) Ethidium bromide-stained, agarose gel electrophoretic separation of amplicons generated using primers A/D (panel A) from chromosomal DNA templates from strains TS559 and Δ TK0808 results in a \sim 190 bp smaller amplicon from *T. kodakarensis* strains lacking TK0808 than the parental strain, TS559. (C) Southern analysis confirms the genome structures of *T. kodakarensis* strains TS559 and Δ TK0808. Probes were generated with primers E/F (left) and B/C (right). M = DNA markers, in bp. (D) Growth curves of *T. kodakarensis* strains TS559 and Δ TK0808, alone and when containing plasmid pTHH6. The moving average (period = 2) is shown as a trend line for each curve.

dynamic as their amide sites accumulated deuterium on the time scale of hours. These HDX-MS results are in accord with the quaternary structure of the PCNA2 trimer (Figure 6B).

The HDX-MS data and protein dynamics of PCNA2 can be compared with those reported previously for the β -subunit of *E. coli* DNA polymerase III (41). While these species serve analogous cellular functions, they differ in that PCNA2 forms a homotrimer in solution, while the β -subunit forms a homodimer (4,17). At long exchange time (>2 h) HDX-MS data observed for the β -subunit exhibits EX1 exchange kinetics patterns (41). In contrast, our data exhibits only EX2 kinetics patterns for PCNA2 at the longest HDX time (1 h) [these mechanisms are outlined in (42)]. We note that the β -subunit data were obtained at 25°C and the data for PCNA2 were measured at 3°C; thus, we cannot rule out temperature as a controlling variable for the differing kinetic behavior. Also, given that PCNA and β -

subunit are different molecules, they may manifest different structural dynamics.

Binding interfaces between PCNA2 and TIP

HDX-MS has the potential to reveal binding interfaces in the protein complex by detecting changes in deuterium uptake rates among backbone amides in response to the formation of the protein complex (43–45). Pairwise comparisons of PCNA2 (PCNA2 trimer alone) and PCNA2 complexed to TIP (PCNA2–TIP complex) and TIP and TIP complexed to PCNA2 provide information regarding the interfaces located on PCNA2 and TIP that stabilize the TIP–PCNA2 complex.

The HDX-MS results for the PCNA2–TIP complex (PCNA monomer:TIP monomer = 1:1) show that peptide region 187–204 of native PCNA2 (Figure 7A and Supplementary Figure S5), located outside of the ring structure, exchanges significantly less deuterium ($P \leq 0.01$, where any value of $P < 0.05$ is considered significant) upon TIP bind-

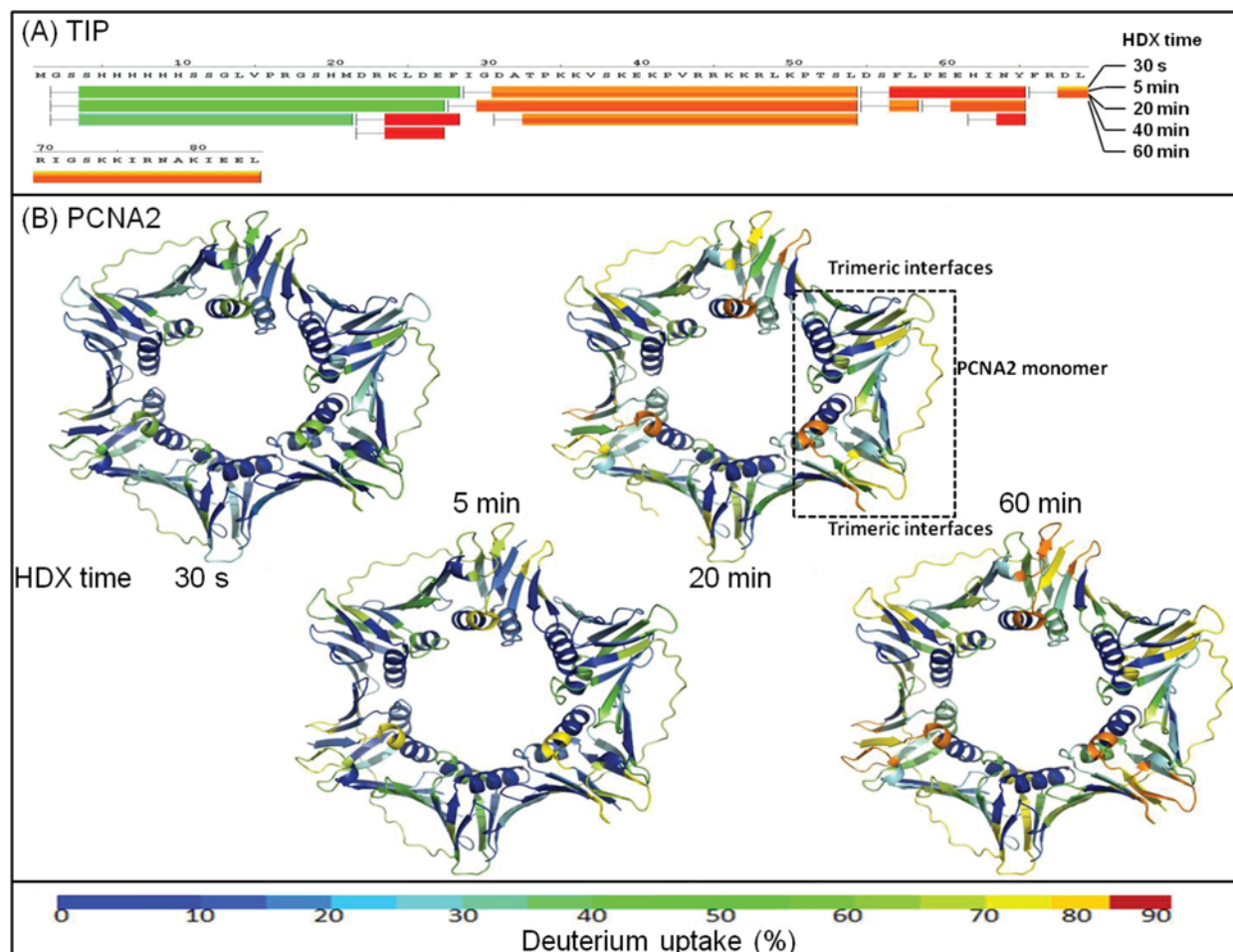


Figure 6. Protein dynamics of PCNA2 and TIP. (A) The observed HDX kinetic results with TIP are plotted according to its peptide sequence. The level of relative deuterium uptake from low to high is indicated with color ranging from blue to red, respectively. (B) The observed HDX kinetic results with native PCNA2 were plotted onto the crystal structure (PDB: 3LX2) (20).

ing. The diminished exchange rate exhibited by peptide region 187–204 in native PCNA2 suggests that these amides are involved in PCNA2–TIP binding. We also observed minor diminished D-uptake rates of peptide region 243–259 of native PCNA2 upon TIP binding (data not shown). However, we regard this observation more cautiously because the 243–259 region comprises mostly the His-tag; thus, the observed decrease in solvent accessibility at this region may be caused by non-specific interactions. Interestingly, peptide regions 34–38 and 104–110 of native PCNA2 exchange more deuterium upon TIP binding (Figure 7A and Supplementary Figure S5), indicating diminished protection factors. Because these amides are located at the trimer interfaces, the diminished protection factors suggest that binding to TIP facilitates the dissociation of PCNA2 trimer.

Although both PCNA1 and PCNA2 bind TIP, mtPCNA does not (Figure 1). After identifying the region at 187–204 in PCNA2 as a potential binding interface in TIP binding, this region was compared in the three PCNAs. PCNA1 and PCNA2 share 59% identity in this region (10/17 residues), mtPCNA shares 23% identity (4/17 residues) with PCNA1 and shares 27% identity (5/18 residues) with PCNA2 (Supplementary Figure S6). The low similarity between mt-

PCNA and PCNA1 and PCNA2 in the region required for TIP binding may explain the inability of mtPCNA to bind TIP.

Mutational analysis of PCNA2–TIP interactions

Based on the HDX-MS results, region 187–204 of PCNA2 was selected for site-directed mutagenesis to examine its role in regulating PCNA2–TIP interaction. Three residues in this region, K197, Y200 and Y204, were mutated to Ala (Figure 8B, PCNA2-A) or Glu (Figure 8B, PCNA2-E). First, the influence of these mutations on the regulation of PCNA by TIP was evaluated using the Fen1 activity assay (Figure 8A). Both PCNA2-A and PCNA2-E stimulate the PCNA-dependent activity of Fen1 (Figure 8C compare lanes 3, 9 and 15 to lane 2; also see panel D) indicating that these mutations did not substantially affect the interactions between PCNA and Fen1. When TIP was added to the reactions, the stimulatory effect of PCNA2-A on Fen1 activity was inhibited to a similar extent as observed with wild-type PCNA protein (Figure 8C compare lanes 10–14 to lanes 4–8; also see panel D). However, the inhibitory effects of TIP on PCNA2-E were substantially reduced (Figure 8C com-

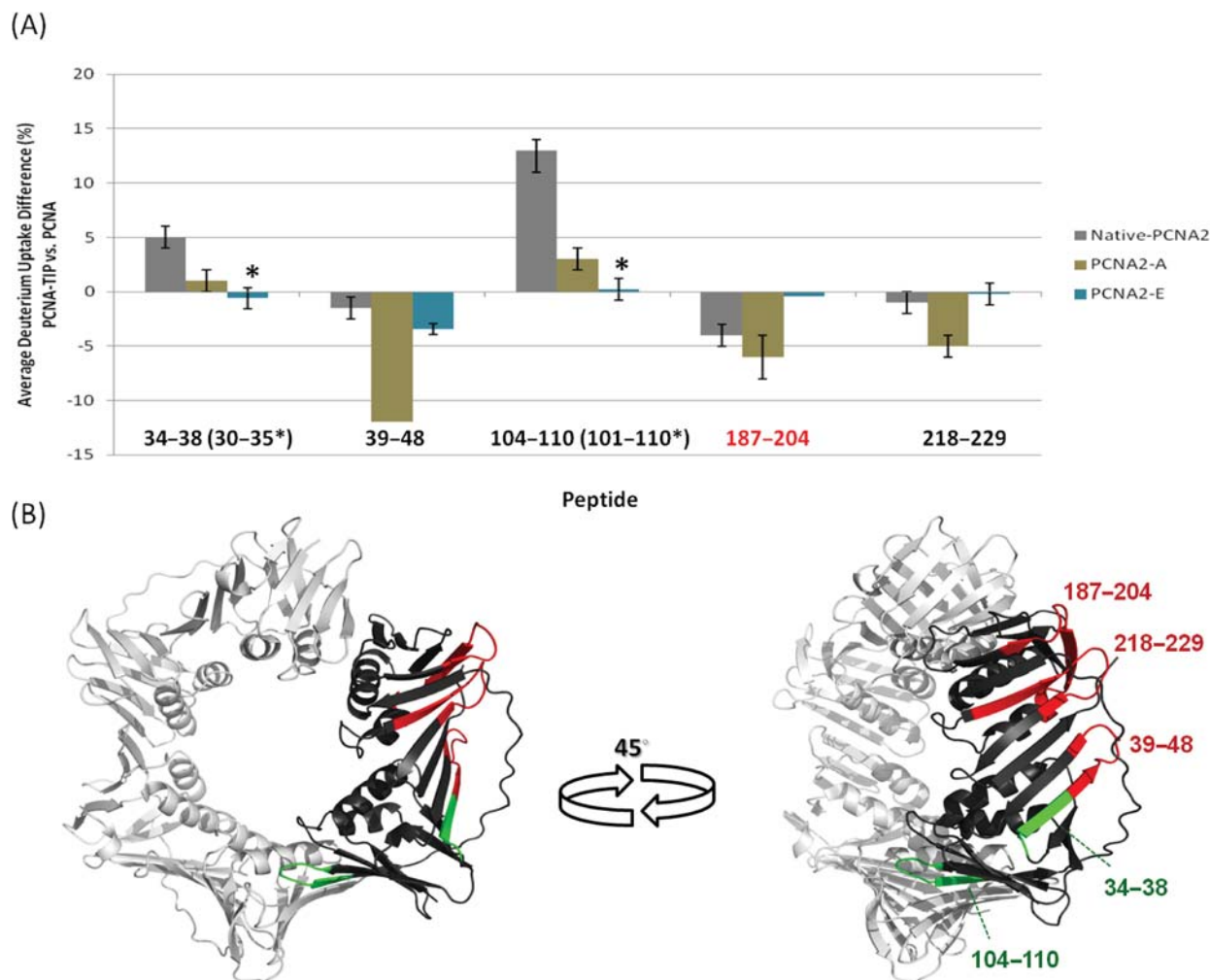


Figure 7. Mutations in PCNA2 affect its interaction with TIP. **(A)** For each peptide (sequence listed below) each colored bar plots the difference ratio (%) between the deuterium uptake by the TIP-PCNA2 complex relative to uncomplexed PCNA2. Colors correspond to the native (gray), A-mutant (olive green) and E-mutant (aqua) PCNA2 proteins. Each bar was computed from the average deuterium uptake found at five HDX time points, and a bracket (thin lines) denotes its standard deviation (1 s). Asterisks on the colored bars of PCNA2-E indicate data originating from slightly shorter peptides. The 187-204 peptide (red) contains sites subjected to mutagenesis. Each plotted peptide group exhibits statistically significant differential peptide data, as inferred by paired *t*-tests (Supplementary Table S2). **(B)** The location of each peptide is shown on the PCNA crystal structure (PDB: 3LX2) (20). Regions showing decreased deuterium uptake in the TIP-PCNA2 complex are colored red, while regions showing increased deuterium uptake are colored green.

pare lanes 16-20 to lanes 4-8; also see panel D) suggesting a weaker interaction between TIP and the PCNA mutant. However, on size exclusion chromatography analysis TIP did not bind to either PCNA2-A or PCNA2-E (Supplementary Figure S7). We also attempted to use several peptides derived from TIP to inhibit PCNA-dependent Fen1 stimulation. However, none of the peptides either alone or in combination inhibited the activity.

The influence of the mutations in PCNA on the TIP-PCNA interactions was then evaluated using HDX-MS. The PCNA2-A mutant showed significant decreases in rate of deuterium uptake not only in region 187-204, but also in regions 39-48 and 218-229 (Figure 7A and Supplementary Figure S8). These regions are composed of short loops that are geometrically close to each other (blue regions in Figure 7), suggesting potential binding interfaces. The HDX-MS results for the PCNA2-A mutant suggest that these mutations strengthen the PCNA2-TIP interactions. Stronger

interaction between the two proteins is supported by the observation that TIP has a stronger inhibitory effect on PCNA2-A stimulation of Fen1 at low TIP concentrations (Figure 8D). Surprisingly, the PCNA2-E mutant showed significant decrease of deuterium uptake only in region 39-48 (Figure 7A and Supplementary Figure S9). The absence of a deuterium uptake difference in region 187-204 underscores the importance of this region in modulating the PCNA2-TIP interactions.

Turning to an examination of the differential deuterium uptake of TIP and the TIP-PCNA2 complex, we noted that peptide regions 22-28 and 55-58 of the TIP-PCNA2 complex (Figure 9A and Supplementary Figure S10A) show slow deuterium uptake rates in the native PCNA2-TIP complex, suggesting potential binding interfaces on TIP in TIP-PCNA2 interaction. Moreover, the HDX kinetics data show that the deuterium uptake of peptide regions 22-28 and 55-58 of TIP in the presence of native PCNA2 eventu-

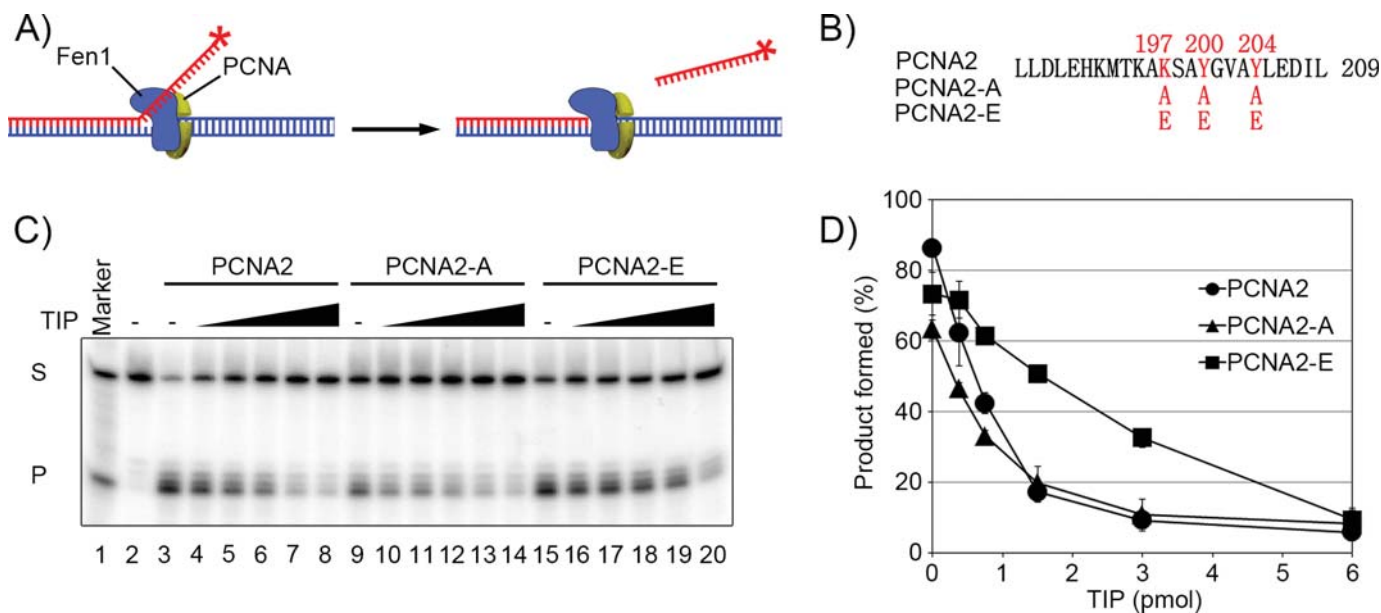


Figure 8. Effect of TIP on the stimulation of Fen1 activity by mutant PCNAs. (A) A schematic illustration of the assay. (B) The residue mutated in PCNA2-A and PCNA2-E. (C) The effect of TIP on the stimulation of Fen1 activity by PCNA wild-type and mutant PCNAs was measured as described in 'Materials and Methods' section in a reaction mixture (20 μ l) that contained 20 fmol substrates, 250 fmol Fen1, 1500 fmol PCNA2 (lanes 3–8), PCNA2-A (lanes 9–14), PCNA2-E (lanes 15–20), in the presence of 375 fmol (lanes 4, 10 and 16), 750 fmol (lanes 5, 11 and 17), 1500 fmol (lanes 6, 12 and 18), 3000 fmol (lanes 7, 13 and 19), or 6000 fmol (lanes 8, 14 and 20) of TIP. Oligonucleotides of 49 nt and 13 nt were separated in lane 1 and marked as 'S' and 'P', respectively. Reaction mixtures were incubated at 60°C for 60 min and the products separated on 10% (w/v) polyacrylamide–8 M urea gels, visualized and quantified by phosphorimaging. A representative gel is shown in panel (C) and the averages with standard deviations from three independent experiments are shown in panel (D).

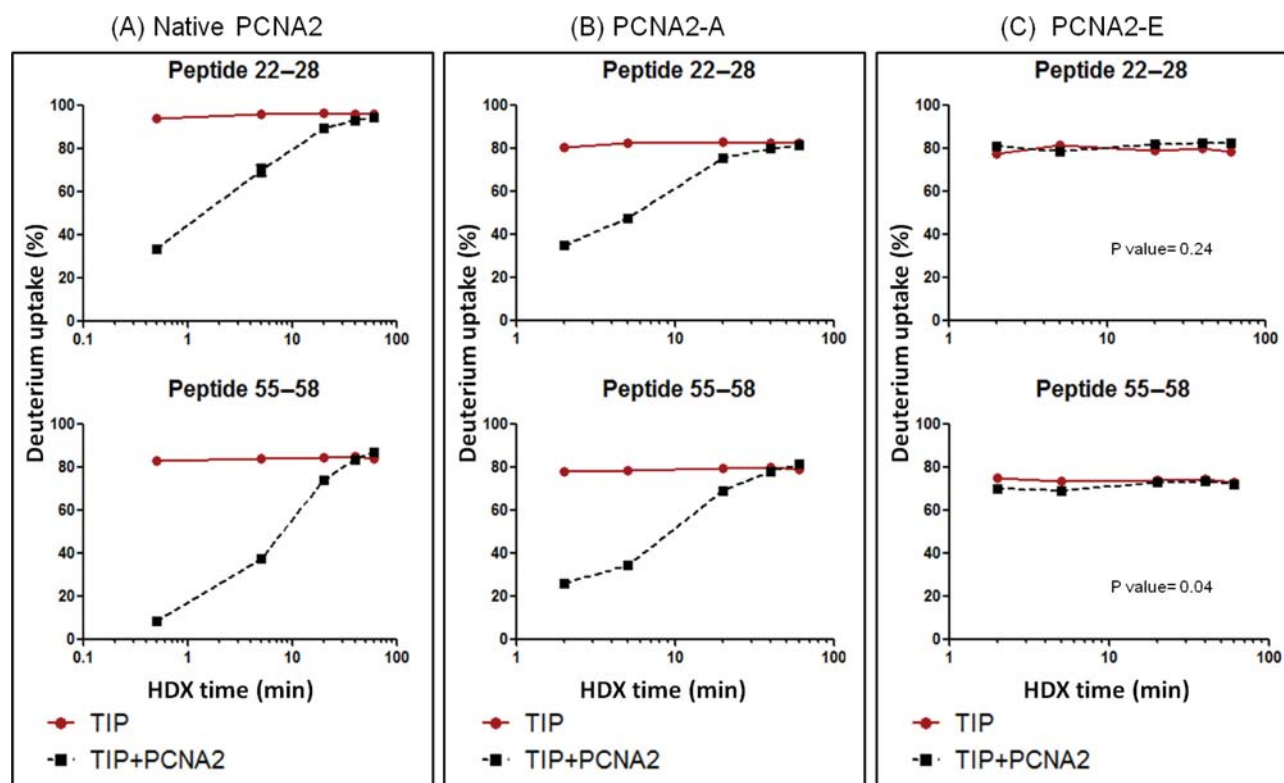


Figure 9. Mutation in PCNA2 affects its interactions with TIP. HDX differences of TIP (red curves) versus the TIP–PCNA2 complex (black curves). Regions of TIP that showed significant differences in D uptake upon binding of native PCNA2 binding are shown in (A). The HDX kinetics of the same regions of TIP in the presence of PCNA2-A mutant and PCNA2-E mutant are plotted in (B) and (C), respectively.

ally reaches the same level as that observed with TIP alone, indicating the flexible nature of the TIP structure. Not surprisingly, our results for the PCNA2-A mutant–TIP complex exhibit a similar trend of HDX kinetics in regions 22–28 and 55–58 of TIP (Figure 9B and Supplementary Figure S10B) as compared with the native PCNA2–TIP complex (Figure 9A). This similarity is in keeping with the formation of a stable PCNA2-A–TIP complex. In contrast, TIP alone and PCNA2-E mutant–TIP complex exhibit no significant difference in deuterium uptake behaviors (Figure 9C and Supplementary Figure S10C), indicating that the PCNA2-E mutant interaction with TIP is weak. In summary, our HDX analyses of PCNA2–TIP complexes show the importance of region 187–204 in regulating the PCNA2–TIP interactions.

DISCUSSION

PCNA plays an essential role in many cellular processes, and thus, the protein requires tight spatial and temporal regulation. In eukarya, a number of mechanisms have been shown to regulate PCNA functions. Post-translational modifications, such as phosphorylation, acetylation, ubiquitination and sumoylation were found to regulate PCNA activity [reviewed in (3,46)]. Binding of small regulatory proteins represents another means to regulate the eukaryotic PCNA; e.g. the cell cycle regulator p21 binds to the IDCL, and prevents PIP-containing proteins from associating with PCNA [e.g. (47)]. Although PCNA modification has not yet been reported in archaea, the presence of protein kinases and small-molecule modifiers in archaea [reviewed in (48,49)] may suggest that similar mechanisms that regulate PCNA may also exist in this domain.

The results presented here identified a new mechanism by which PCNA proteins are regulated. Binding of TIP to PCNA does not involve a PIP motif, KA motif or any other known motif shown to be involved in PCNA binding. It also does not involve the IDCL or the C-terminal part of PCNA, which has been shown to participate in PCNA binding by different proteins. Our results suggest that TIP binds to the interface between the monomers of the trimeric ring and contributes to ring dissociation or other structural changes that inhibit PCNA-dependent activities. Although homologues of TIP have been identified only in Thermococcales, other species may also contain small proteins that bind PCNA and affect the integrity of the PCNA ring.

Although PCNA is expressed in all cell types and has a long half-life, the protein is highly expressed in tumor cells. In fact, PCNA was first identified in patients with systemic lupus erythematosus (50). It was suggested that PCNA could be an important target for cancer therapy [e.g. (51)]. A number of small molecules that inhibit PCNA have been developed, most of which target the IDCL, thus preventing PCNA interaction with enzymes that contain a PIP motif [e.g. (52)]. The structures of PCNA from all organisms are similar (5) and therefore it is possible that the data presented here may provide a new mechanism for PCNA inhibition. Our data suggest that one may design small molecules that mimic TIP and bind PCNA in the same region, resulting in the dissociation of the trimeric ring and suppression of PCNA activity.

ACCESSION NUMBER

PDB: 3LX2.

SUPPLEMENTARY DATA

Supplementary Data are available at NAR online.

ACKNOWLEDGMENTS

We would like to thank Dr Jane Ladner for her suggestion leading to the construction of the monomeric forms of proliferating cell nuclear antigen. Certain commercial materials, instruments and equipments are identified in this paper in order to specify the experimental procedure as completely as possible. These identifications do not imply a recommendation or endorsement by the National Institute of Standards and Technology nor does it imply that the materials, instruments, or equipments are the best for the purpose.

FUNDING

National Science Foundation [MCB-0815646 to Z.K.]; National Institutes of Health [GM098176, GM100329 to T.J.S., GH034559 to J.H.]. Source of open access funding: National Institute of Standards and Technology intramural funds.

Conflict of interest. None declared.

REFERENCES

- Vivona, J.B. and Kelman, Z. (2003) The diverse spectrum of sliding clamp interacting proteins. *FEBS Lett.*, **546**, 167–172.
- Moldovan, G.L., Pfander, B. and Jentsch, S. (2007) PCNA, the maestro of the replication fork. *Cell*, **129**, 665–679.
- Stoimenov, I. and Helleday, T. (2009) PCNA on the crossroad of cancer. *Biochem. Soc. Trans.*, **37**, 605–613.
- Jeruzalmi, D., O'Donnell, M. and Kuriyan, J. (2002) Clamp loaders and sliding clamps. *Curr. Opin. Struct. Biol.*, **12**, 217–224.
- Indiani, C. and O'Donnell, M. (2006) The replication clamp-loading machine at work in the three domains of life. *Nat. Rev. Mol. Cell Biol.*, **7**, 751–761.
- Kelman, Z. and Hurwitz, J. (1998) Protein–PCNA interactions: a DNA-scanning mechanism? *Trends Biochem. Sci.*, **23**, 236–238.
- Winter, J.A. and Bunting, K.A. (2012) Rings in the extreme: PCNA interactions and adaptations in the archaea. *Archaea*, **2012**, 951010.
- Yao, N.Y. and O'Donnell, M. (2012) The RFC clamp loader: structure and function. *Subcell Biochem.*, **62**, 259–279.
- Warbrick, E. (1998) PCNA binding through a conserved motif. *Bioessays*, **20**, 195–199.
- Warbrick, E., Heatherington, W., Lane, D.P. and Glover, D.M. (1998) PCNA binding proteins in *Drosophila melanogaster*: the analysis of a conserved PCNA binding domain. *Nucleic Acids Res.*, **26**, 3925–3932.
- Gulbis, J.M., Kelman, Z., Hurwitz, J., O'Donnell, M. and Kuriyan, J. (1996) Structure of the C-terminal region of p21^{WAF1/CIP1} complexed with human PCNA. *Cell*, **87**, 297–306.
- Xu, H., Zhang, P., Liu, L. and Lee, M.Y. (2001) A novel PCNA-binding motif identified by the panning of a random peptide display library. *Biochemistry*, **40**, 4512–4520.
- Haracska, L., Acharya, N., Unk, I., Johnson, R.E., Hurwitz, J., Prakash, L. and Prakash, S. (2005) A single domain in human DNA polymerase ϵ mediates interaction with PCNA: implications for translesion DNA synthesis. *Mol. Cell Biol.*, **25**, 1183–1190.
- Kelman, Z., Zuo, S., Arroyo, M.P., Wang, T.S. and Hurwitz, J. (1999) The C-terminal region of *Schizosaccharomyces pombe* proliferating cell nuclear antigen is essential for DNA polymerase activity. *Proc. Natl. Acad. Sci. U.S.A.*, **96**, 9515–9520.
- Gomes, X.V. and Burgers, P.M. (2000) Two modes of FEN1 binding to PCNA regulated by DNA. *EMBO J.*, **19**, 3811–3821.

16. Gilljam, K.M., Feyzi, E., Aas, P.A., Sousa, M.M., Muller, R., Vagbo, C.B., Catterall, T.C., Liabakk, N.B., Slupphaug, G., Drablos, F. *et al.* (2009) Identification of a novel, widespread, and functionally important PCNA-binding motif. *J. Cell Biol.*, **186**, 645–654.
17. Kelman, Z. and O'Donnell, M. (1995) Structural and functional similarities of prokaryotic and eukaryotic DNA polymerase sliding clamps. *Nucleic Acids Res.*, **23**, 3613–3620.
18. Dalrymple, B.P., Kongsuwan, K., Wijffels, G., Dixon, N.E. and Jennings, P.A. (2001) A universal protein–protein interaction motif in the eubacterial DNA replication and repair systems. *Proc. Natl. Acad. Sci. U.S.A.*, **98**, 11627–11632.
19. Kurz, M., Dalrymple, B., Wijffels, G. and Kongsuwan, K. (2004) Interaction of the sliding clamp beta-subunit and Hda, a DnaA-related protein. *J. Bacteriol.*, **186**, 3508–3515.
20. Ladner, J.E., Pan, M., Hurwitz, J. and Kelman, Z. (2011) Crystal structures of two active proliferating cell nuclear antigens (PCNAs) encoded by *Thermococcus kodakaraensis*. *Proc. Natl. Acad. Sci. U.S.A.*, **108**, 2711–2716.
21. Pan, M., Santangelo, T.J., Čuboňová, L., Li, Z., Metangmo, H., Ladner, J., Hurwitz, J., Reeve, J.N. and Kelman, Z. (2013) *Thermococcus kodakaraensis* has two functional PCNA homologues but only one is required for viability. *Extremophiles*, **17**, 453–461.
22. Kuba, Y., Ishino, S., Yamagami, T., Tokuhara, M., Kanai, T., Fujikane, R., Daiyasu, H., Atomi, H. and Ishino, Y. (2012) Comparative analyses of the two proliferating cell nuclear antigens from the hyperthermophilic archaeon, *Thermococcus kodakaraensis*. *Genes Cells*, **17**, 923–937.
23. Pan, M., Kelman, L.M. and Kelman, Z. (2011) The archaeal PCNA proteins. *Biochem. Soc. Trans.*, **39**, 20–24.
24. Li, Z., Santangelo, T.J., Čuboňová, L., Reeve, J.N. and Kelman, Z. (2010) Affinity purification of an archaeal DNA replication protein network. *MBio*, **1**, e00221–00210.
25. Shen, Y., Musti, K., Hiramoto, M., Kikuchi, H., Kawarabayashi, Y. and Matsui, I. (2001) Invariant Asp-1122 and Asp-1124 are essential residues for polymerization catalysis of family D DNA polymerase from *Pyrococcus horikoshii*. *J. Biol. Chem.*, **276**, 27376–27383.
26. Chemnitz Galal, W., Pan, M., Kelman, Z. and Hurwitz, J. (2012) Characterization of the DNA primase complex isolated from the archaeon, *Thermococcus kodakaraensis*. *J. Biol. Chem.*, **287**, 16209–16219.
27. Kelman, Z. and Hurwitz, J. (2000) A unique organization of the protein subunits of the DNA polymerase clamp loader in the archaeon *Methanobacterium thermoautotrophicum* DH. *J. Biol. Chem.*, **275**, 7327–7336.
28. Shin, J.-H., Jiang, Y., Grabowski, B., Hurwitz, J. and Kelman, Z. (2003) Substrate requirements for duplex DNA translocation by the eukaryal and archaeal minichromosome maintenance helicases. *J. Biol. Chem.*, **278**, 49053–49062.
29. Hileman, T.H. and Santangelo, T.J. (2012) Genetics techniques for *Thermococcus kodakaraensis*. *Front. Microbiol.*, **3**, 195.
30. Sato, T., Fukui, T., Atomi, H. and Imanaka, T. (2005) Improved and versatile transformation system allowing multiple genetic manipulations of the hyperthermophilic archaeon *Thermococcus kodakaraensis*. *Appl. Environ. Microbiol.*, **71**, 3889–3899.
31. Santangelo, T.J., Cubonova, L. and Reeve, J.N. (2010) *Thermococcus kodakaraensis* genetics: TK1827-encoded beta-glycosidase, new positive-selection protocol, and targeted and repetitive deletion technology. *Appl. Environ. Microbiol.*, **76**, 1044–1152.
32. Cubonova, L., Katano, M., Kanai, T., Atomi, H., Reeve, J.N. and Santangelo, T.J. (2012) An archaeal histone is required for transformation of *Thermococcus kodakaraensis*. *J. Bacteriol.*, **194**, 6864–6674.
33. Čuboňová, L., Richardson, T., Burkhart, B.W., Kelman, Z., Reeve, J.N., Connolly, B.A. and Santangelo, T.J. (2013) Archaeal DNA polymerase D but not DNA polymerase B is required for genome replication in *Thermococcus kodakaraensis*. *J. Bacteriol.*, **195**, 2322–2328.
34. Pascal, B.D., Willis, S., Lauer, J.L., Landgraf, R.R., West, G.M., Marciano, D., Novick, S., Goswami, D., Chalmers, M.J. and Griffin, P.R. (2012) HDX workbench: software for the analysis of H/D exchange MS data. *J. Am. Soc. Mass Spectrom.*, **23**, 1512–1521.
35. Press, W.H. (2007) *Numerical Recipes: The Art of Scientific Computing*, 3rd edn. Cambridge University Press, Cambridge, UK; New York.
36. Hubscher, U. and Seo, Y.S. (2001) Replication of the lagging strand: a concert of at least 23 polypeptides. *Mol. Cells*, **12**, 149–157.
37. Balakrishnan, L. and Bambara, R.A. (2013) Okazaki fragment metabolism. *Cold Spring Harb. Perspect. Biol.*, **5**, a010173.
38. Bae, S.H., Bae, K.H., Kim, J.A. and Seo, Y.S. (2001) RPA governs endonuclease switching during processing of Okazaki fragments in eukaryotes. *Nature*, **412**, 456–461.
39. Burgers, P.M. and Yoder, B.L. (1993) ATP-independent loading of the proliferating cell nuclear antigen requires DNA ends. *J. Biol. Chem.*, **268**, 19923–19926.
40. Rand, K.D., Zehl, M., Jensen, O.N. and Jorgensen, T.J. (2009) Protein hydrogen exchange measured at single-residue resolution by electron transfer dissociation mass spectrometry. *Anal. Chem.*, **81**, 5577–5584.
41. Fang, J., Engen, J.R. and Beuning, P.J. (2011) *Escherichia coli* processivity clamp beta from DNA polymerase III is dynamic in solution. *Biochemistry*, **50**, 5958–5968.
42. Englander, S.W. (2006) Hydrogen exchange and mass spectrometry: a historical perspective. *J. Am. Soc. Mass Spectrom.*, **17**, 1481–1489.
43. Chalmers, M.J., Busby, S.A., Pascal, B.D., West, G.M. and Griffin, P.R. (2011) Differential hydrogen/deuterium exchange mass spectrometry analysis of protein-ligand interactions. *Expert Rev. Proteomics*, **8**, 43–59.
44. Huang, R. Y., Garai, K., Frieden, C. and Gross, M.L. (2011) Hydrogen/deuterium exchange and electron-transfer dissociation mass spectrometry determine the interface and dynamics of apolipoprotein E oligomerization. *Biochemistry*, **50**, 9273–9282.
45. Huang, R. Y., Wen, J., Blankenship, R.E. and Gross, M.L. (2012) Hydrogen-deuterium exchange mass spectrometry reveals the interaction of Fenna-Matthews-Olson protein and chlorosome CsmA protein. *Biochemistry*, **51**, 187–193.
46. Jackson, S.P. and Durocher, D. (2013) Regulation of DNA damage responses by ubiquitin and SUMO. *Mol. Cell*, **49**, 795–807.
47. Gibbs, E., Kelman, Z., Gulbis, J.M., O'Donnell, M., Kuriyan, J., Burgers, P.M.J. and Hurwitz, J. (1997) The influence of the proliferating cell nuclear antigen-interacting domain of p21^{CIP1} on DNA synthesis catalyzed by the human and *Saccharomyces cerevisiae* polymerase delta holoenzymes. *J. Biol. Chem.*, **272**, 2373–2381.
48. Kennelly, P.J. (2003) Archaeal protein kinases and protein phosphatases: insights from genomics and biochemistry. *Biochem. J.*, **370**, 373–389.
49. Maupin-Furlow, J.A. (2013) Ubiquitin-like proteins and their roles in archaea. *Trends Microbiol.*, **21**, 31–38.
50. Miyachi, K., Fritzler, M.J. and Tan, E.M. (1978) Autoantibody to a nuclear antigen in proliferating cells. *J. Immunol.*, **121**, 2228–2234.
51. Tan, Z., Wortman, M., Dillehay, K.L., Seibel, W.L., Evelyn, C.R., Smith, S.J., Malkas, L.H., Zheng, Y., Lu, S. and Dong, Z. (2012) Small-molecule targeting of proliferating cell nuclear antigen chromatin association inhibits tumor cell growth. *Mol. Pharmacol.*, **81**, 811–819.
52. Punchihewa, C., Inoue, A., Hishiki, A., Fujikawa, Y., Connelly, M., Evison, B., Shao, Y., Heath, R., Kuraoka, I., Rodrigues, P. *et al.* (2012) Identification of small molecule proliferating cell nuclear antigen (PCNA) inhibitor that disrupts interactions with PIP-box proteins and inhibits DNA replication. *J. Biol. Chem.*, **287**, 14289–14300.

SUPPLEMENTARY INFORMATION

Supplementary Figure S1. TIP does not interact with mtPCNA monomers. Proteins (100 μg each) were separated on a Superdex-200 gel filtration column as described in “Materials and Methods”. Aliquots (80 μl) from the indicated fractions were separated on 15% SDS-PAGE and stained with Coomassie brilliant blue (R-250). A. mtPCNA; B. mtPCNA_m; C. TIP; D. mtPCNA and TIP; E, mtPCNA_m and TIP.

Supplementary Figure S2. TIP affects the interactions of PCNA1 and PCNA2 with PolB. Proteins (100 μg each) were separated on a Superdex-200 gel filtration column as described in “Materials and Methods”. Aliquots (80 μl) from the indicated fractions were separated on 15% SDS-PAGE and followed by Coomassie brilliant blue (R-250) staining. A. PCNA1; B. PCNA2; C. TIP; D, PolB; E, PCNA1 and PolB; F, PCNA1, PolB and TIP; G, PCNA2 and PolB; H, PCNA2, PolB and TIP; I, PolB and TIP.

Supplementary Figure S3. Total ion chromatogram of peptides obtained from PCNA1 (top) and PCNA2 (bottom) through on-line digestion platform. PCNA1 showed poor digestion efficiency and mainly yielded the undigested protein.

Supplementary Figure S4. Peptic peptides of native PCNA2 and TIP. An on-line digestion device provides 98% sequence coverage of PCNA2 (A) and 99% sequence coverage of TIP (B) (53).

Supplementary Figure S5. Differential HDX map of wild-type PCNA2 in which the regions having negative values of deuterium uptake difference (PCNA2 vs. TIP-PCNA2 complex) suggest that the protein conformation changes toward a more protected conformation upon the binding of TIP.

Supplementary Figure S6. Alignment of the residues on PCNA involved in TIP binding. Residues 187-204 in PCNA2 are aligned with the region in PCNA1 and mtPCNA proteins. Amino acids which are identical in two out of the three proteins are highlighted

in red.

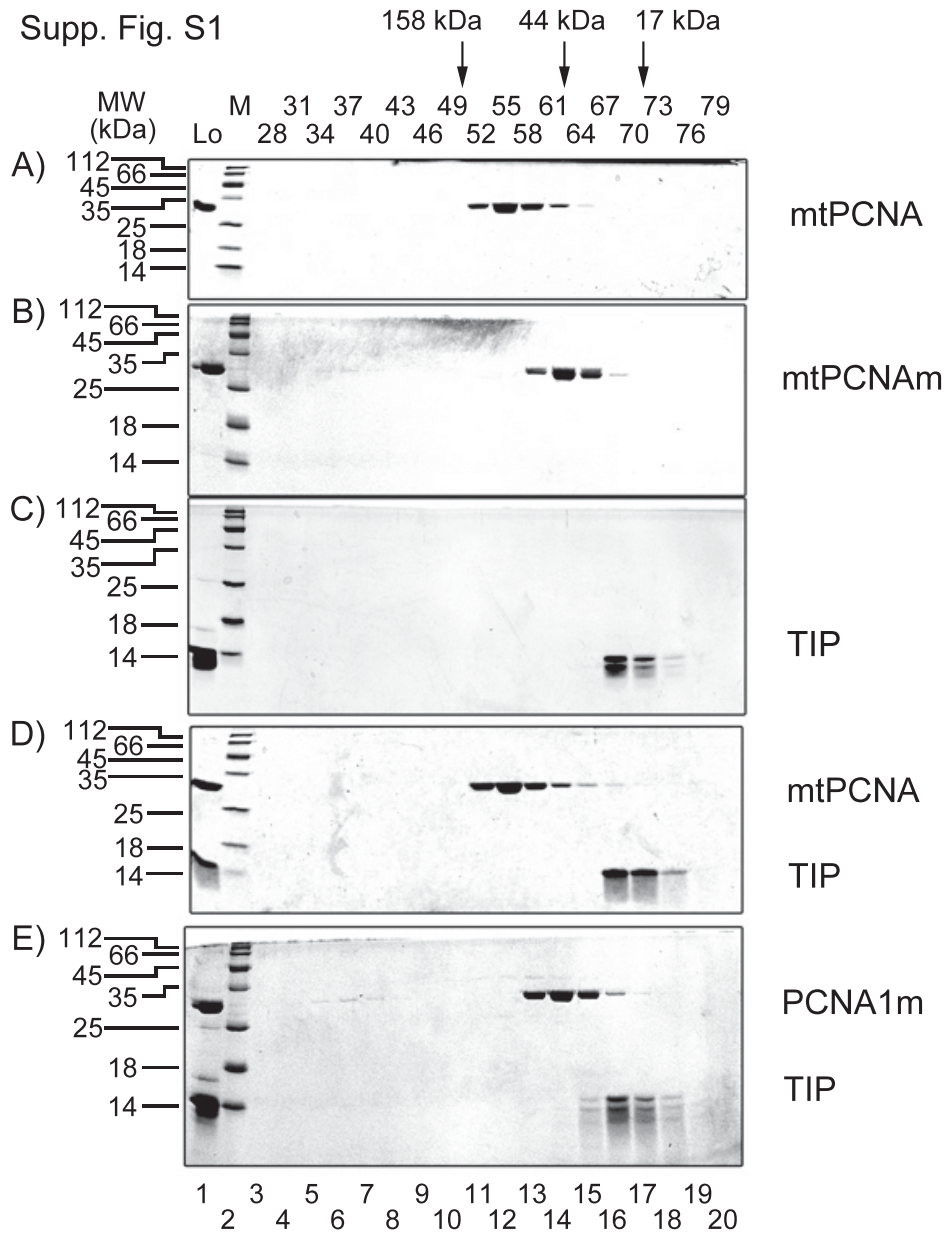
Supplementary Figure S7. TIP does not interact with PCNA2-A and PCNA2-E. Proteins (100 µg each) were separated on a Superdex-200 gel filtration column as described in “Materials and Methods”. Aliquots (80 µl) from the indicated fractions were separated on 15% SDS-PAGE and stained with Coomassie brilliant blue (R-250). A. PCNA2-E; B. PCNA2-E and TIP; C. PCNA2-A; D. PCNA2-A and TIP.

Supplementary Figure S8. Differential HDX map of the PCNA2-A mutant in which the regions having negative values of deuterium uptake difference (PCNA2-A mutant vs. TIP-PCNA2-A mutant complex) suggest that the protein conformation changes toward a more protected conformation upon the binding of TIP.

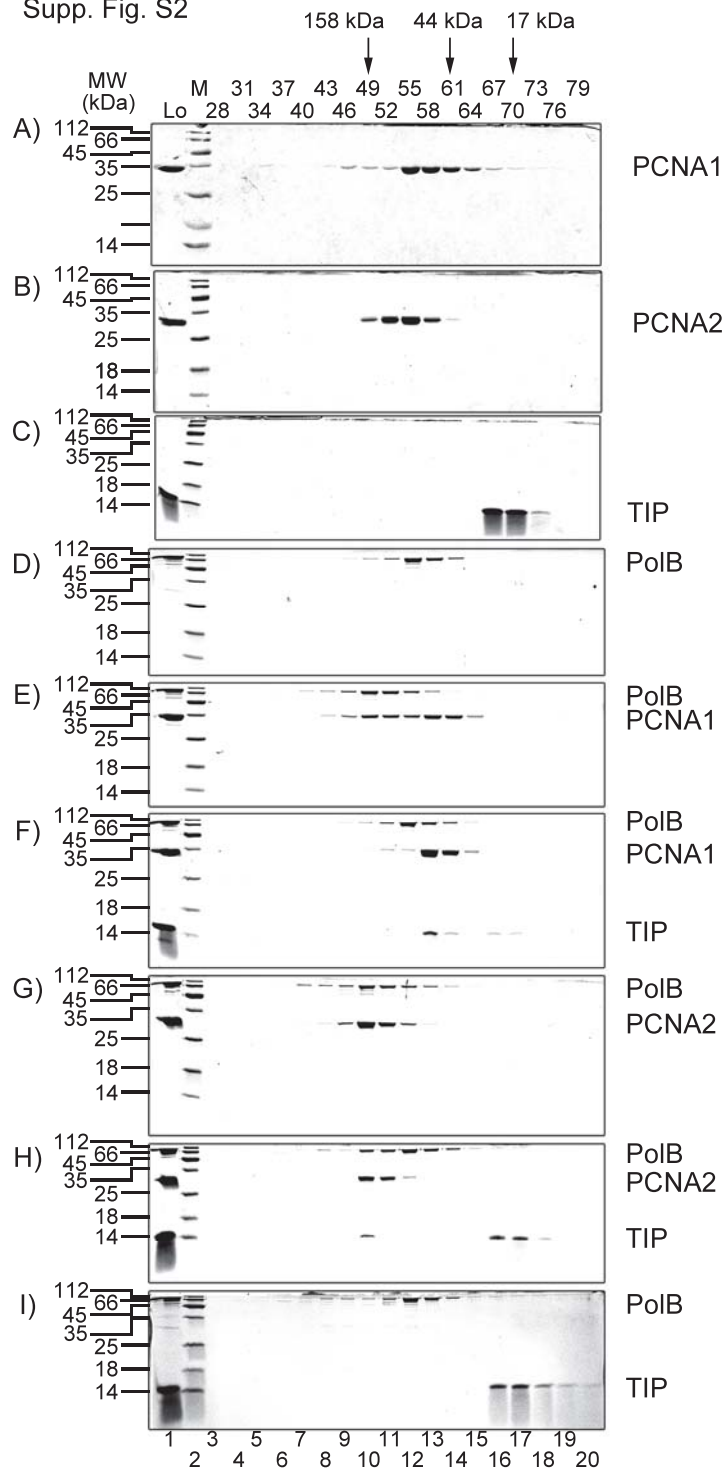
Supplementary Figure S9. Differential HDX map of the PCNA2-E mutant in which the regions having negative values of deuterium uptake difference (PCNA2-E mutant vs. TIP-PCNA2-E mutant complex) suggest that the protein conformation changes toward a more protected conformation upon the binding of TIP.

Supplementary Figure S10. Differential HDX map of TIP in which the regions having negative values of deuterium uptake difference (TIP vs. TIP-PCNA2 complex) suggest that the protein conformation changes toward a more protected conformation upon the binding of native PCNA2 (A), PCNA2-A mutant (B), and PCNA2-E mutant (C).

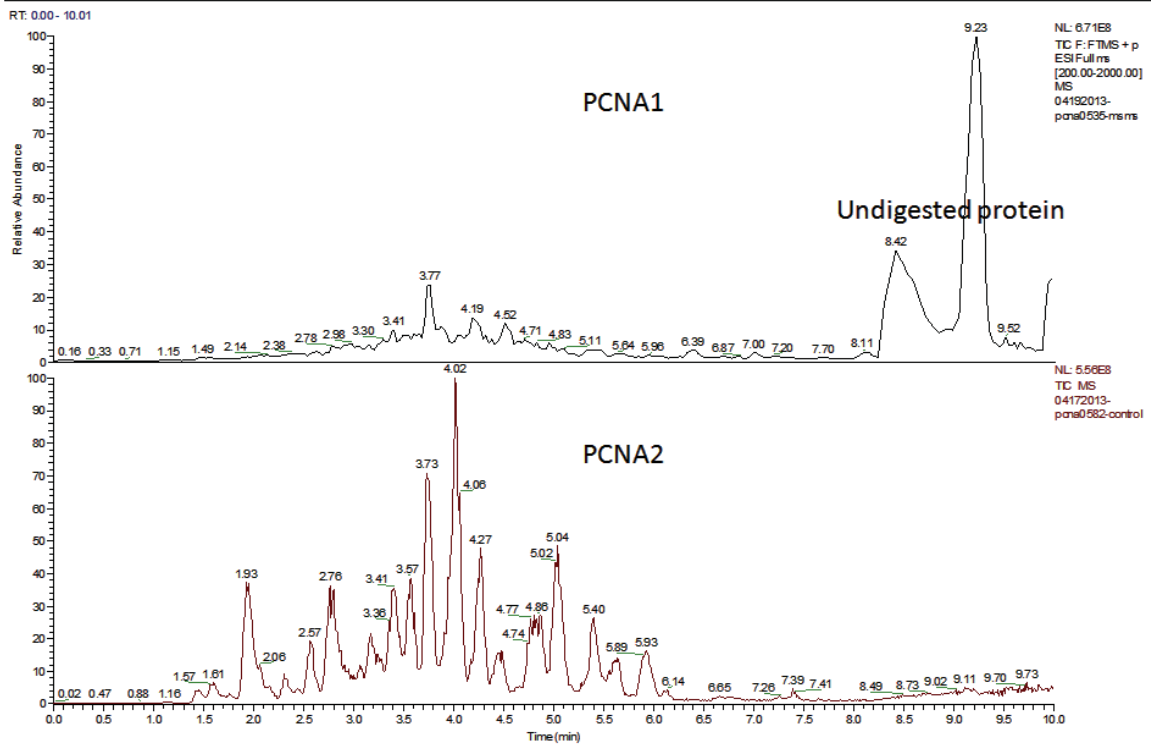
Supp. Fig. S1



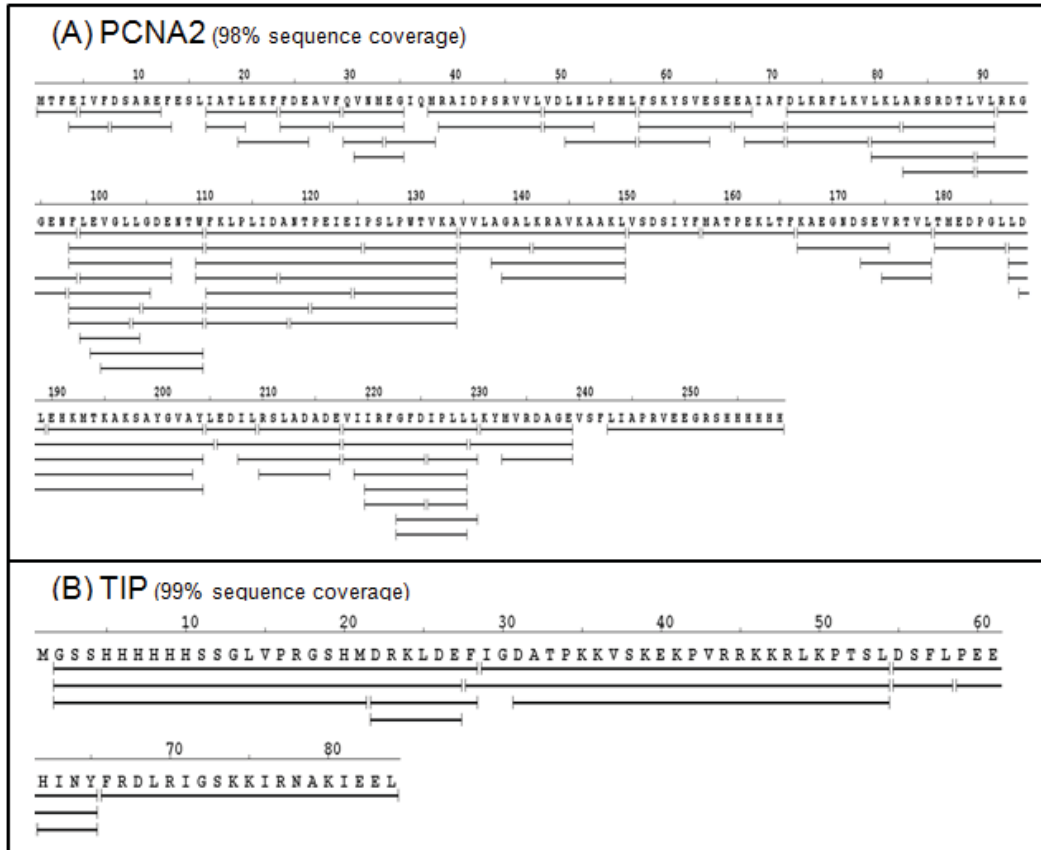
Supp. Fig. S2



Supp. Fig. S3

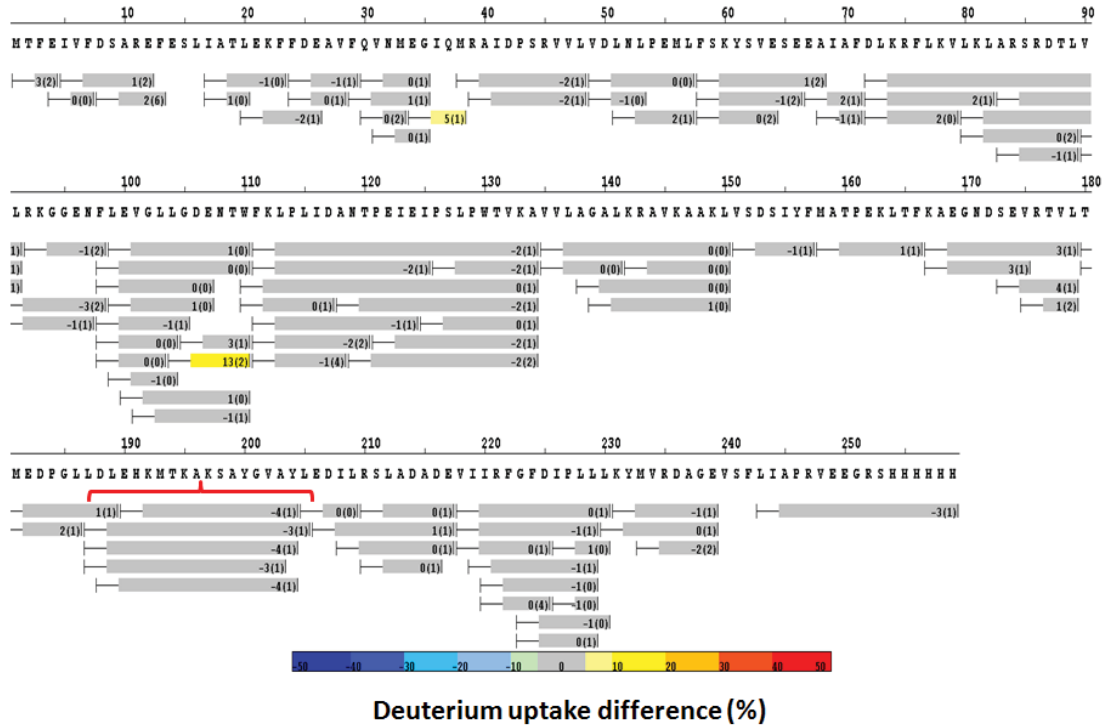


Supp. Fig. S4



Supp. Fig. S5

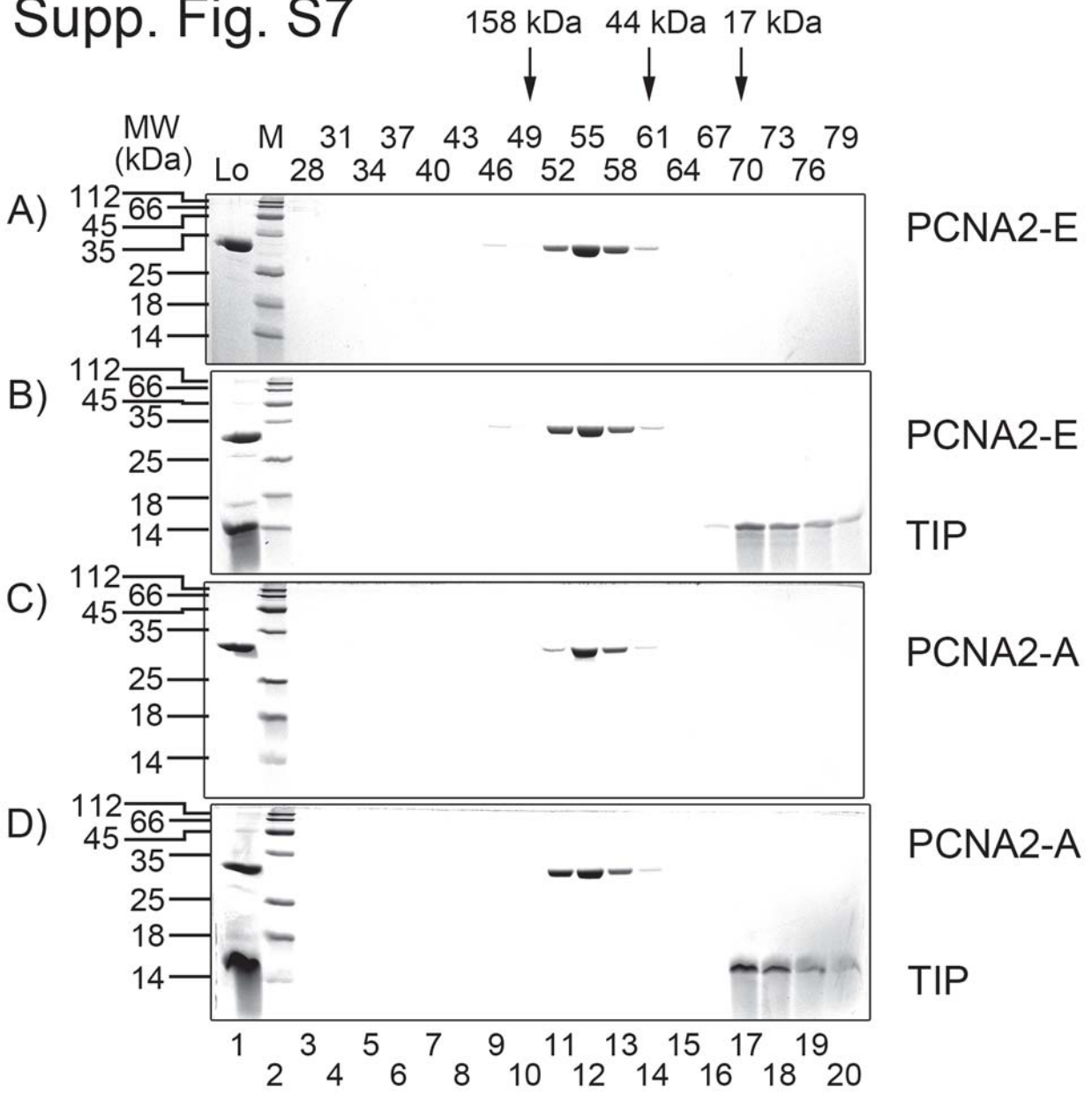
Native PCNA2_HDX Protection (Ligand: TIP)



Supp. Fig. S6

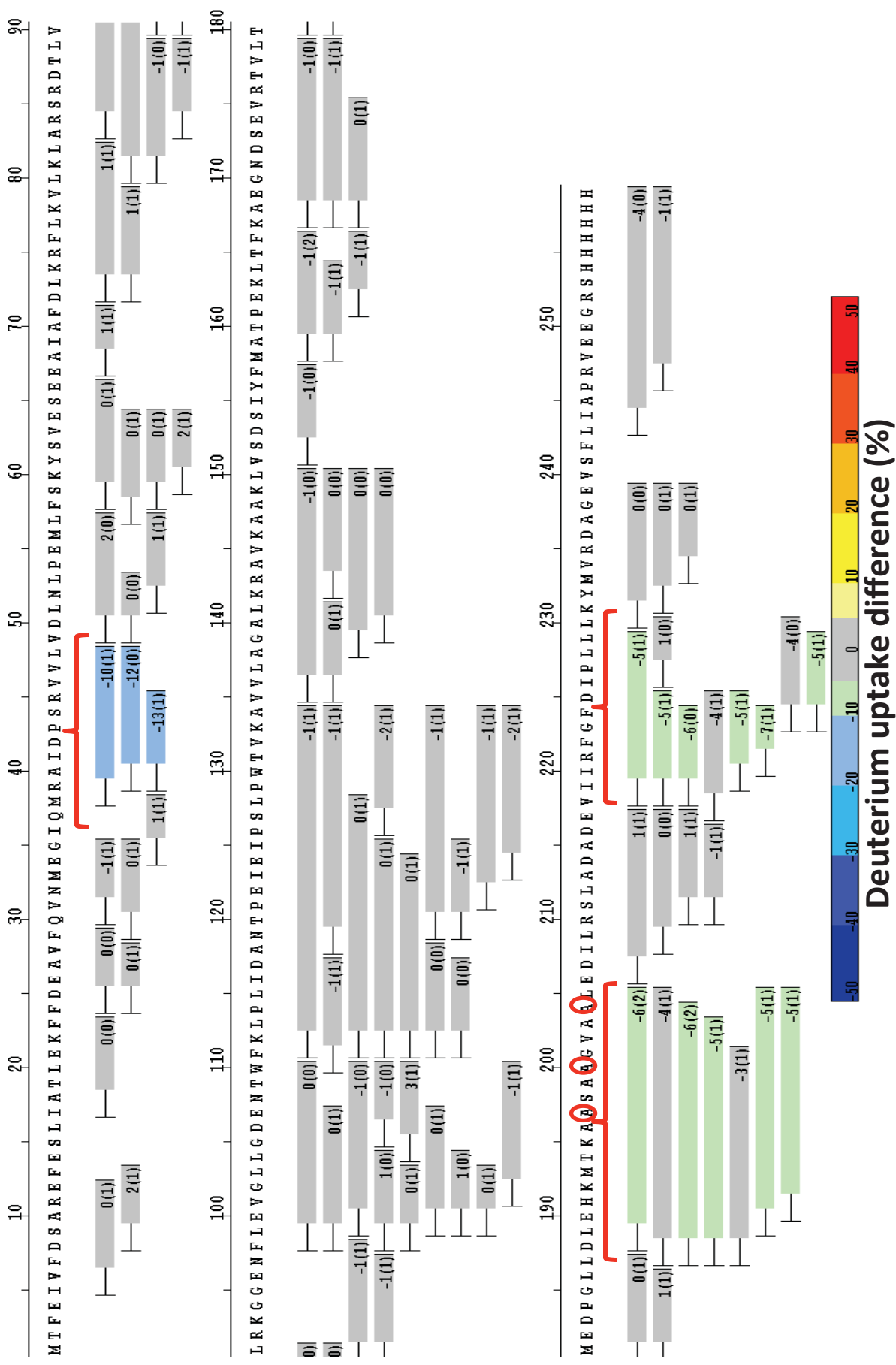
PCNA1	187	LDLEVE-EETKSAYGIRY	203
PCNA2	187	LDLEHKMTKAKSAYGVAY	204
mtPCNA	178	LHGERIDKPARSIYSLDK	195

Supp. Fig. S7



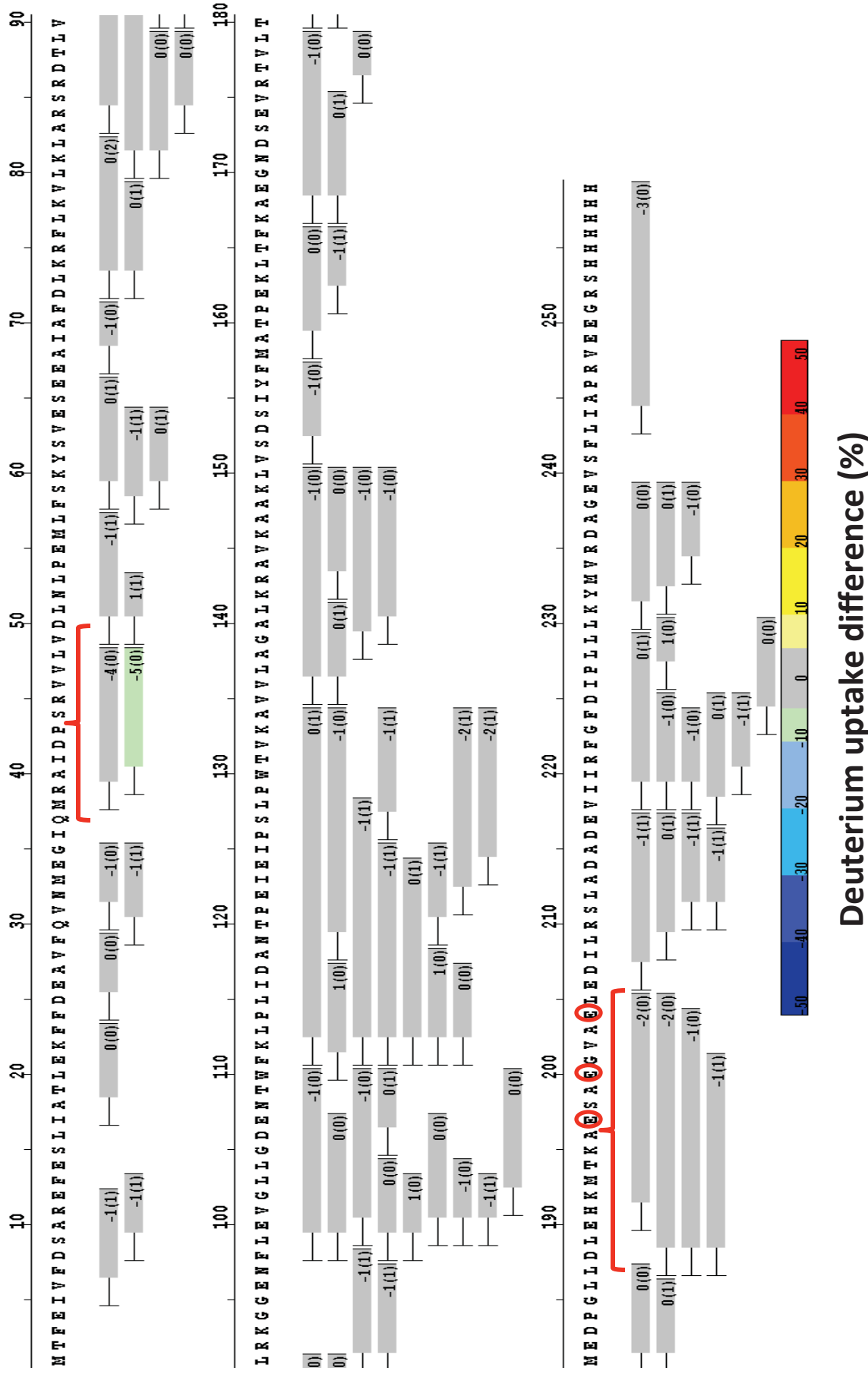
PCNA2-A_HDX Protection (Ligand: TIP)

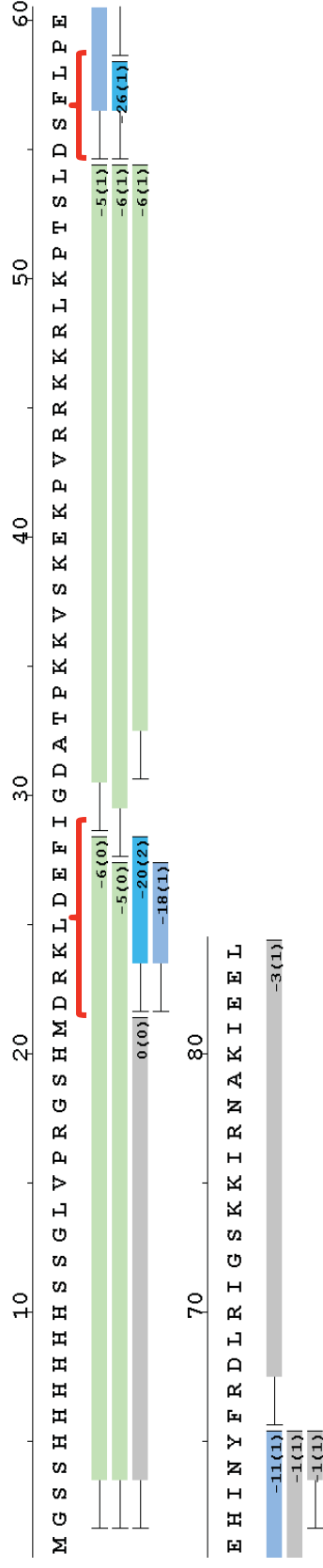
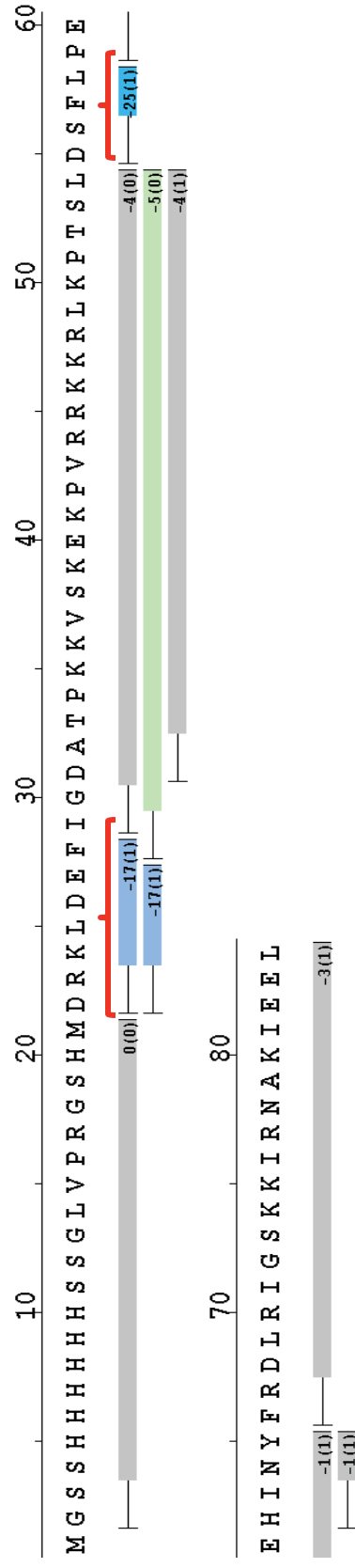
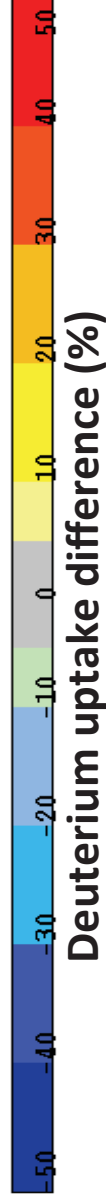
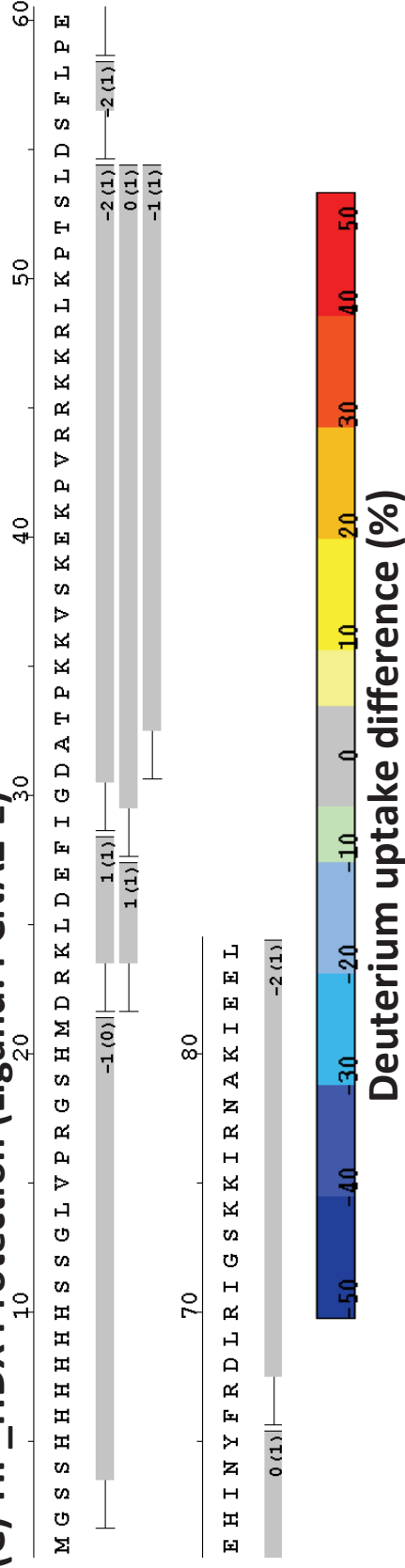
Supp. Fig. S8



PCNA2-E_HDX Protection (Ligand: TIP)

Supp. Fig. S9



(A) TIP_HDX Protection (Ligand: Native PCNA2)**(B) TIP_HDX Protection (Ligand: PCNA2-A)****(C) TIP_HDX Protection (Ligand: PCNA2-E)**

Supplementary Table S1. Oligonucleotides used for cloning and mutagenesis

Name	Used to generate	Sequence
Zhuo_0498	PCNA2-A	5'-AGATGACAAAAGCGGCCAGTGCGGCCGGGGTTGCAGCCCTC-3'
Zhuo_0499	PCNA2-A	5'-GAGGGCTGCAACCCCGGCCGCACTGGCCGCCCTTTGTCATCT-3'
Zhuo_0500	PCNA2-E	5'-AGATGACAAAAGCGGAAAGTGCGGAAAGGGGTTGCAGAACTCGAGGACATC-3'
Zhuo_0501	PCNA2-E	5'-GATGTCCTCGAGTTCTGTCAACCCCTTCCGCACCTTCCGCCCTTGTCACTCT-3'
Zhuo_0395	Fen1	5'-ATGCCATATGGGAGTCCAGATAGGTGAGC-3'
Zhuo_0396	Fen1	5'-AATTGTCGACCTATCGACCCGAACCAAGCTCTC-3'
Zhuo_0277	TIP	5'-ATGCCATATGGACAGGAAGCTCGACGAG-3'
Zhuo_0278	TIP	5'-GTACGTCGACTTATAACTCCTCGATTTTCGCG-3'
Zhuo_0502	TK0535 E143K	5'-CCTCGGTGAGGTTCTCAAGAAGGCATAAAGGACGCTT-3'
Zhuo_0503	TK0535 E143K	5'-AAGCGTCCTTTATGCCCTTCTTGAGAACCTCACCCGAGG-3'
Zhuo_0504	TK0535 V175D-I177K	5'-GCGAGACCAACGAGGACGAGAAGAGGCTTACCCTTGAGGA-3'
Zhuo_0505	TK0535 V175D-I177K	5'-TCCTCAAGGGTAAGCCCTCTTCTCGTCCCTCGTTGGTCTCCG-3'

Supplementary Table S2. P values obtained from paired t-test of five HDX time points of PCNA2 vs. PCNA2+TIP.

PCNA2 vs. PCNA2+TIP

PCNA2

Peptide	34-38	39-48	104-110	187-204	218-119
P value	<0.01	0.04	<0.01	0.01	0.05

PCNA2-A

Peptide	34-38	39-48	104-110	187-204	218-119
P value	0.19	<0.01	<0.01	<0.01	<0.01

PCNA2-E

Peptide	30-35	39-48	101-110	187-204	218-119
P value	0.06	<0.01	0.97	0.06	0.07